AWARD NUMBER: W81XWH-13-1-0107

TITLE: Uncovering the Role of BMP Signaling in Melanocyte Development and Melanoma Tumorigenesis

PRINCIPAL INVESTIGATOR: Craig J. Ceol

CONTRACTING ORGANIZATION: University of Massachusetts Medical School
Worcester, MA 01605-2300

REPORT DATE: September 2016

TYPE OF REPORT: Final

PREPARED FOR: U.S. Army Medical Research and Materiel Command
Fort Detrick, Maryland 21702-5012

REPORT DOCUMENTATION PAGE

Form Approved
OMB No. 0704-0188

1. REPORT DATE	2. REPORT TYPE	3. DATES COVERED
September 2016	Final	1-JUL-2013 TO 30-JUN-2016

4. TITLE AND SUBTITLE

Uncovering the Role of BMP Signaling in Melanocyte Development and Melanoma Tumorigenesis

5a. CONTRACT NUMBER

5b. GRANT NUMBER
W81XWH-13-1-0107

5c. PROGRAM ELEMENT NUMBER

6. AUTHOR(S)
Craig J. Ceol, Ph.D.

E-Mail: Craig.Ceol@umassmed.edu

5d. PROJECT NUMBER

5e. TASK NUMBER

5f. WORK UNIT NUMBER

7. PERFORMING ORGANIZATION NAME(S) AND ADDRESS(ES)
University of Massachusetts Medical School
55 Lake Avenue
Worcester, MA 01655-0002

8. PERFORMING ORGANIZATION REPORT NUMBER

9. SPONSORING / MONITORING AGENCY NAME(S) AND ADDRESS(ES)

U.S. Army Medical Research and Materiel Command
Fort Detrick, Maryland 21702-5012

10. SPONSOR/MONITOR'S ACRONYM(S)

11. SPONSOR/MONITOR'S REPORT NUMBER(S)

12. DISTRIBUTION / AVAILABILITY STATEMENT

Approved for Public Release; Distribution Unlimited

13. SUPPLEMENTARY NOTES

14. ABSTRACT

Melanoma is the most aggressive and lethal form of skin cancer. In 2013 over 75,000 Americans were diagnosed with melanoma, and nearly 10,000 died from this disease. It has been known for over a decade that mutations that overactivate the *BRAF* and *NRAS* genes promote melanoma formation. At the same time it has also become clear that these mutations are not sufficient for melanoma formation and other genes are involved. Using genomic studies and cross-species comparisons, we identified the BMP factor *GDF6* as a gene that may cooperate with mutant *BRAF* to promote melanoma. The aims of this grant are to determine if *GDF6* does in fact cooperate with mutant *BRAF* and uncover the mechanisms by which *GDF6* acts in melanomas and normal melanocytes. Toward these aims, we have used our zebrafish model to demonstrate cooperativity between *GDF6* and mutant *BRAF* in accelerating melanoma onset. Furthermore, we have knocked down *GDF6* in human melanoma cells, finding that loss of *GDF6* causes cells to cease proliferating. These and other data suggest that *GDF6* promotes melanoma progression and its withdrawal is detrimental to melanoma cell growth. We are currently investigating whether blocking *GDF6* function is a viable therapeutic strategy.

15. SUBJECT TERMS

Nothing listed

16. SECURITY CLASSIFICATION OF:			17. LIMITATION OF ABSTRACT	18. NUMBER OF PAGES	19a. NAME OF RESPONSIBLE PERSON
a. REPORT	b. ABSTRACT	c. THIS PAGE			USAMRMC
Unclassified	Unclassified	Unclassified	Unclassified	101	19b. TELEPHONE NUMBER *(include area code)*

Table of Contents

Page

INTRODUCTION:

Melanoma is the most aggressive skin cancer, and every year it kills nearly 10,000 Americans and roughly 60,000 people worldwide. A greater understanding of the genetic basis for melanoma is essential for designing new ways to diagnose and treat this disease. Nearly a decade ago, it was discovered that mutations that inappropriately activate the *BRAF* gene are present in over half of all human melanomas. Activated *BRAF* mutations are necessary for formation of these melanomas, but numerous studies have shown that they are not sufficient. To find other genes that cooperate with *BRAF* in creating melanomas, we have used genomic studies and cross-species comparisons to identify several candidates. One of these candidates, *GDF6*, is a BMP factor that is recurrently amplified and upregulated in human and zebrafish melanomas. The purpose of this study is to functionally analyze the role of *GDF6* in melanoma progression. In addition, this study aims to use gain and loss of function studies to determine how *GDF6* acts in melanomas and normal melanocytes. A major goal of this research is to determine if *GDF6* can be used as a diagnostic or prognostic marker in melanoma and is a potential therapeutic target.

KEYWORDS:
cancer, melanoma, melanocyte, bone morphogenetic protein, GDF6, BRAF, neural crest

ACCOMPLISHMENTS:

Major goals of the project (as described in Statement of Work):

Task 1: Perform gain and loss of function studies in zebrafish embryos and mammalian cultured cells to determine if GDF6 antagonizes melanocyte development.

Task 2: Use established screening procedures in zebrafish to determine if GDF6 overexpression accelerates melanoma onset or exacerbates other properties of melanomas. In addition, use human melanoma cells to determine if GDF6 knockdown in GDF6-positive cells or overexpression in GDF6-minus cells affects tumorigenicity.

Task 3: Use BMP pathway reporters to determine the dynamics of BMP activity in normal melanocytes and melanoma cells. Examine GDF6 expression and mutation status in human melanomas, benign melanocytic lesions and normal melanocytes to determine if modulation of GDF6 activity is consistent with a role in melanoma formation.

Accomplishments under these goals:

Task 1

In this task, studies in zebrafish and mammalian cultured cells were proposed to determine the effects of *gdf6b* overexpression and *gdf6b* loss on melanocyte development. Zebrafish expressing *gdf6b* in melanocyte progenitors fail to develop melanocytes, suggesting that *gdf6b* inhibits terminal differentiation of melanocytes. We have examined zebrafish with mutation in *gdf6a*. *gdf6a* mutant embryos have excess melanocytes as do embryos treated with the BMP inhibitor DMH1 (Fig. 1A,B). We are combining the existing *gdf6a* mutant with a mutant we obtained for *gdf6b* and will be examining these embryos for supernumerary melanocytes. Together these results indicate that *gdf6* paralogs, via BMP signaling, play an important role in restricting melanocyte development during embryogenesis.

Experiments in cultured human melanoma cells suggest that *gdf6* genes inhibit melanocyte development by promoting a neural crest identity. In these experiments we performed expression profiling of melanoma cells with a loss of *GDF6* activity as compared to those with a gain in BMP signaling activity (Fig. 2A). Differentially regulated genes were subjected to biological pathway analysis, and the pathways most significantly regulated by *GDF6* were ossification and neural crest (Fig. 2B). *GDF6* promoted expression of trunk neural crest genes (e.g. *SOX10*) but inhibited expression of cranial neural crest genes (e.g. *SOX9*) (Fig. 2C). Based on these results we hypothesized that *GDF6* promotes a neural crest identity in melanoma cells, enabling these cells to remain less differentiated, survive and proliferate. As part this analysis we discovered that the *MITF* gene, the master regulator of melanocyte development, is regulated by *GDF6*. Specifically, *MITF* expression is repressed by *GDF6* (Fig. 3A). Through chromatin immunoprecipitation with next generation sequencing (ChIPseq) we discovered that phosphoSMAD1/5/8, which are downstream effectors of *GDF6*, bind to the *MITF* locus (Fig.3B). When *GDF6* is knocked down, binding of phosphoSMAD1/5/8 is reduced (Fig. 3B,C), *MITF* expression is increased, and melanoma cells begin to differentiate. We also probed the role of *GDF6* in repressing *SOX9* expression. Upon *GDF6* knockdown, we found that *SOX9* expression increased (Fig. 4A). Since *SOX9* is a pro-apoptotic factor in melanomas, we asked whether the cell death that occurred upon *GDF6* knockdown was dependent on *SOX9*. Indeed elimination of *SOX9* prevented the death that was caused by *GDF6* knockdown and enabled tumor growth even when *GDF6* was knocked down (Fig. 4B,C). Thus, *GDF6* promotes a trunk neural crest identity that involves repression of *MITF* and *SOX9* to prevent differentiation and cell death. Together with the results described above, it is likely that a normal developmental role of *GDF6* genes in regulating neural crest and melanocyte development is reiterated to promote tumor initiation and progression.

Task 2

To address this task, a zebrafish screening scheme, termed the 'MiniCoopR' assay, was used to determine if *gdf6b* has an effect on melanoma progression. In this assay, melanocyte-deficient animals are injected with DNA that can both rescue melanocytes and overexpress a gene of interest. Zebrafish with

rescued melanocytes are monitored weekly for tumors to determine if the gene of interest affects tumor onset as compared to a control gene. When *gdf6b* was overexpressed using MiniCoopR, melanomas arose more quickly as compared to *EGFP* controls (Fig. 5A). *GDF6* was also expressed in cultured human A375 melanoma cells. *GDF6* overexpressing cells were xenotransplanted into nude mice and tumor progression monitored as compared to control A375 cells. *GDF6* overexpression caused tumors to grow much more quickly than controls (Fig. 5B). A375 and other human melanoma cell lines express endogenous *GDF6*, so we determined the effects of *GDF6* knockdown in these cell lines. When *GDF6* was knocked down using multiple, independent shRNAs A375 and other melanoma cells underwent programmed cell death (Fig. 5C). When knockdown cells were xenotransplanted prior to death, melanoma progression was markedly decreased (Fig. 5D). (Note: no Department of Defense funds were used for xenotransplantation experiments). Taken together, these results indicate that *GDF6* is an oncogene and the cell death resulting from its knockdown makes it an excellent target for anti-melanoma therapy.

Knockdown and overexpression cells are being used to determine how *GDF6* acts. The GDF6 protein is initially made as a proprotein, which is cleaved in cells to generate mature, secreted GDF6. To determine if soluble, mature GDF6 acts as a pro-survival factor, we added media containing mature GDF6 to *GDF6* knockdown cells. GDF6-containing media rescued the effects of *GDF6* knockdown (Fig. 6), indicating that GDF6 can act as a secreted protein to promote melanoma cell survival. These data suggest that targeting soluble, extracellular GDF6 is a therapeutic strategy for melanoma and possibly other types of tumors.

Task 3

A major goal of this task is to assess the effects of *GDF6* on BMP signaling activity. In zebrafish we initially proposed to use a fluorescent reporter to monitor transcriptional output of BMP activity – however, technical difficulties have made this approach untenable. Instead, we have used antibodies that recognized phosphorylated SMAD1/5/8 to measure BMP signaling activity. In zebrafish, melanomas have robust phospho-SMAD expression (Fig. 7A). In cultured melanoma cells we similarly detect GDF6 and phospho-SMAD1/5/8 expression. When *GDF6* is knocked down, phospho-SMAD1/5/8 levels go down (Fig. 7B), consistent with the notion that GDF6 signals through SMAD1/5/8 and the BMP signaling pathway.

Additional experiments were performed to determine if *GDF6* acts via the BMP signaling pathway. Knockdown of *SMAD1* resulted in the same cell death phenotype as *GDF6* knockdown, suggesting that both genes act in the same pathway. To directly assess whether *GDF6* acts via the BMP signaling pathway we performed genetic epistasis analyses. In these epistasis experiments an activated variant of *SMAD1* was used. This variant, *SMAD1DVD*, contains amino acid substitutions in key catalytic residues, resulting in a constitutively active protein. When *GDF6* knockdown was performed in A375 cells expressing *SMAD1DVD*, cell death was suppressed (Fig. 7C), indicating that *GDF6* acts upstream of or in parallel to *SMAD1*. When such cells were xenotransplanted into immunocompromised mice, they grew much more quickly than *GDF6* knockdown cells (Fig. 7D), again indicating that *GDF6* acts upstream of *SMAD1*. (Note: no Department of Defense funds were used for xenotransplantation experiments)

To further study how *GDF6* acts through BMP signaling, we performed ChIPseq using an antibody that recognizes phospho-SMAD1/5/8. In these studies we found that knockdown of *GDF6* led to a diminution of phospho-SMAD1/5/8 binding to DNA (FIg. 3C). These results were reflected in several bound genes, including *MITF* (as described above) as well as the canonical BMP targets *ID1* and *ID3* (Fig. 8A,B).

Stainings of human tissue samples were used to further investigate the role of *GDF6* and BMP signaling in melanoma. Robust expression of GDF6 and phospho-SMAD1/5/8 was observed in human melanoma sections (Fig. 9A,B). To determine if there is a correlation between GDF6 or phospho-SMAD1/5/8 expression and clinical outcome, we stained a tissue microarray of human melanoma tissue cores, each of which has associated clinical data. An analysis of these stainings indicated a correlation between the level of GDF6 expression and patient survival (Fig. 9C). Specifically, patients whose tumors expressed high levels of GDF6 had poor survival as compared to patients whose tumors expressed low of no GDF6. These findings provide a rationale that inhibition of GDF6 could have therapeutic benefit.

Opportunities for training and professional development:

A graduate student in my laboratory, Arvind Venkatesan, conducted the bulk of the experiments described. He and I met regularly, once per week, to design experiments, discuss results, write manuscripts and create public presentations of our work. In each of these activities I served as a mentor to him. During the past reporting

period, Arvind was also able to attend several conferences, including the Zebrafish Disease Models 8 conference in Boston, MA and Connecticut Valley Zebrafish Meetings throughout the northeast.

Dissemination of results:
Portions of this work have been presented at the following venues. Each of these groups included community and/or media members. Primary attendees are listed in parentheses.
• Tufts University American Cancer Society Relay for Life Seminar (local ACS chapter)
• University of Massachusetts Medical School Media Fellowship (local media reporters)
• University of Massachusetts Medical School community outreach (various community organizations)

Plan for next reporting period:
Nothing to Report.

IMPACT:

Impact on the development of the principal discipline:
This project straddles two disciplines – developmental biology and cancer biology. The findings described in this report identify a new role for *GDF6* genes in the development of the melanocyte lineage. The effect on the melanocyte lineage likely stems from *GDF6* activity in the embryonic neural crest, the tissue from which melanocytes are derived. We speculate that *GDF6* normally promotes a neural crest identity in cells, and loss of *GDF6* in embryogenesis causes neural crest cells to more readily adopt a melanocyte fate. Our findings support a model in which this embryonic activity of *GDF6* is reiterated to promote oncogenesis. Specifically, *GDF6* in tumors promotes a neural crest identity, thereby preventing differentiation and cell death. These results highlight a fundamental paradigm in which embryonic activities can be co-opted to promote tumorigenesis.

Impact on other disciplines:
These findings have a potential impact on the discipline of clinical oncology. Since inhibition of *GDF6* can cause death of melanoma cells in culture, we are currently developing approaches to target GDF6 protein. It is a secreted molecule that can potentially be blocked with neutralizing antibodies. We have created a panel of mouse monoclonal antibodies and are currently developing assays to determine whether any inhibit binding of GDF6 to its receptor. Ultimately we aim to develop GDF6-blocking antibodies and test their efficacy as melanoma therapies.

Impact on technology transfer:
We are currently developing blocking antibodies and aim to partner with an industry sponsor to complete pre-clinical studies and begin early-stage clinical trials.

Impact on society beyond science and technology:
Nothing to Report.

CHANGES/PROBLEMS:

Changes in approach and reasons for change:
Nothing to Report.

Actual or anticipated problems or delays and actions or plans to resolve them:
Nothing to Report.

Changes that had a significant impact on expenditures:
Nothing to Report.

Significant changes in use or care of human subjects, vertebrate animals, biohazards, and/or select agents:
Nothing to Report.

PRODUCTS:
This career development award has helped to jump start my activities as an independent researcher. Below are examples of the products and opportunities that have arisen in part because of the funding from the Department of Defense CDMRP. I am very grateful for the support.

Publications, conference papers, and presentations:

Journal publications

• Iyengar, S., Kasheta, M. and Ceol, C.J. (2015). Poised regeneration of zebrafish melanocytes involves direct differentiation and concurrent replenishment of tissue-resident progenitor cells. *Developmental Cell*, *33*, *631-43*.
• Wojciechowska, S., van Rooijen, E., Ceol, C., Patton, E.E. and White, R. (2016). Generation and analysis of zebrafish melanoma models. *Methods in Cell Biology*, in the press.
• Moore, F.E., Garcia, E.G., Lobbardi, R., Jain, E., Tang, Q., Moore, J.C., Cortes, M., Molodtsov, A., Kasheta, M., Luo, C.C., Garcia, A.J., Mylvaganam, R., Yoder, J.A., Blackburn, J.S., Sadreyev, R.I., Ceol, C.J., North, T.E. and Langenau, D.M. (2016). Single-cell transcriptional analysis of normal, aberrant and malignant hematopoiesis in zebrafish. *Journal of Experimental Medicine*, in the press.
• Wojciechowska, S., Zeng, Z., Lister, J.A., Ceol, C.J., Patton, E.E. (2016). Melanoma regression and recurrence in zebrafish. *Methods Molecular Biology*, in the press.
• Venkatesan, A.M., Vyas, R., Dresser, K., Gujja, S., Bhatnagar, S., Chhangawala, S., Gomes, C., Xi, H.S., Lian, C.G., Houvras, Y., Edwards, Y.J.K., Deng, A., Green, M. and Ceol, C.J. (2016). GDF6 ligand-induced BMP signaling induces a neural crest identity and is critical for survival and growth of melanomas. Submitted.

Books or other non-periodical, one-time publications

Nothing to Report.

Other publications, conference papers, and presentations

Conference Talks:
• 52nd Annual Meeting of The American Society of Dermatopathology, San Francisco, CA
• PanAmerican Society for Pigment Cell Research Conference, Irvine, CA
• The Allied Genetics Conference, Orlando, FL
• PanAmerican Society for Pigment Cell Research Conference, Baltimore, MD
Invited seminars:
• Tufts University, Medford, MA
American Cancer Society Relay for Life Seminar
• University of Massachusetts Medical School, Worcester, MA
Division of Hematology/Oncology Grand Rounds
• MassBiologics, Boston, MA
MassBiologics Research Seminar
• Yale University, New Haven, CT
Internal Medicine Seminar Series

Websites or other internet sites

Nothing to Report.

Technologies or techniques

Nothing to Report.

Inventions, patent applications, and/or licenses

Patent application:
• Targeting GDF6 and BMP Signaling for Anti-Melanoma Therapy, US Serial No. 62/130,749

Other products

Nothing to Report.

PARTICIPANTS AND OTHER COLLABORATING ORGANIZATIONS:

Individuals who worked on the project:

Arvind Venkatesan, Graduate Student, UMass Medical School
Craig Ceol, Assistant Professor, UMass Medical School

Change in active other support of the PD/PI since the last reporting period:
Nothing to Report.

Other organizations involved as partners:
Nothing to Report.

SPECIAL REPORTING REQUIREMENTS:
Nothing to Report.

APPENDICES:

Please see appended figures referred to in the Accomplishments section.

Please see appended *curriculum vitae* for Dr. Ceol.

Please see appended manuscript entitled 'Ligand-dependent BMP signaling reawakens an embryonic neural crest identity to promote melanoma', which is currently under review at the journal *Science.*

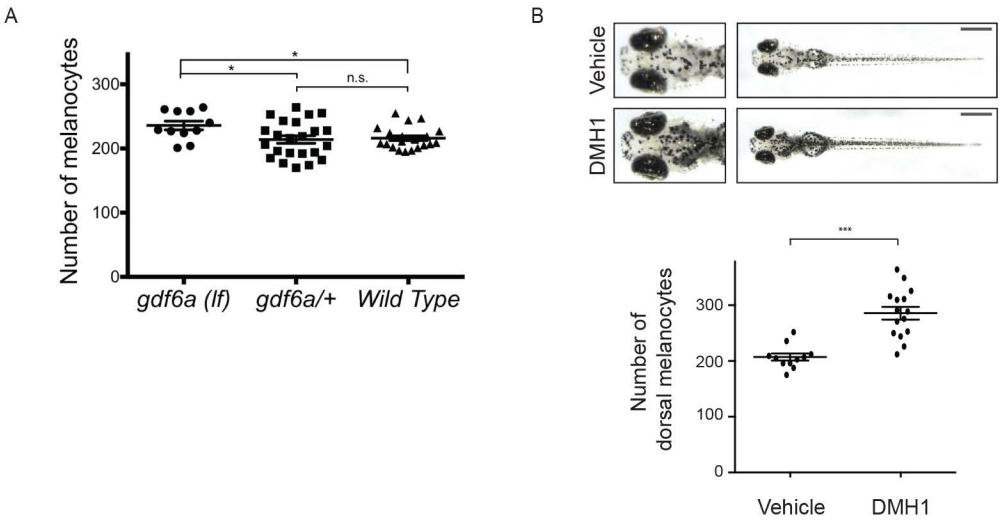

Figure 1
A) gdf6a mutants develop a greater number of melanocytes than wild-type and heterozygous animals. B) Top, epinephrine-treated zebrafish embryos at 5dpf incubated with DMSO vehicle control or 5μM DMH1. Scale bar: 500 μM. Bottom, melanocyte quantification. Error bars indicate s.e.m.; n=3. Two-tailed Student's t-test, *P<0.01, ***P< 0.001. ns, not significant.

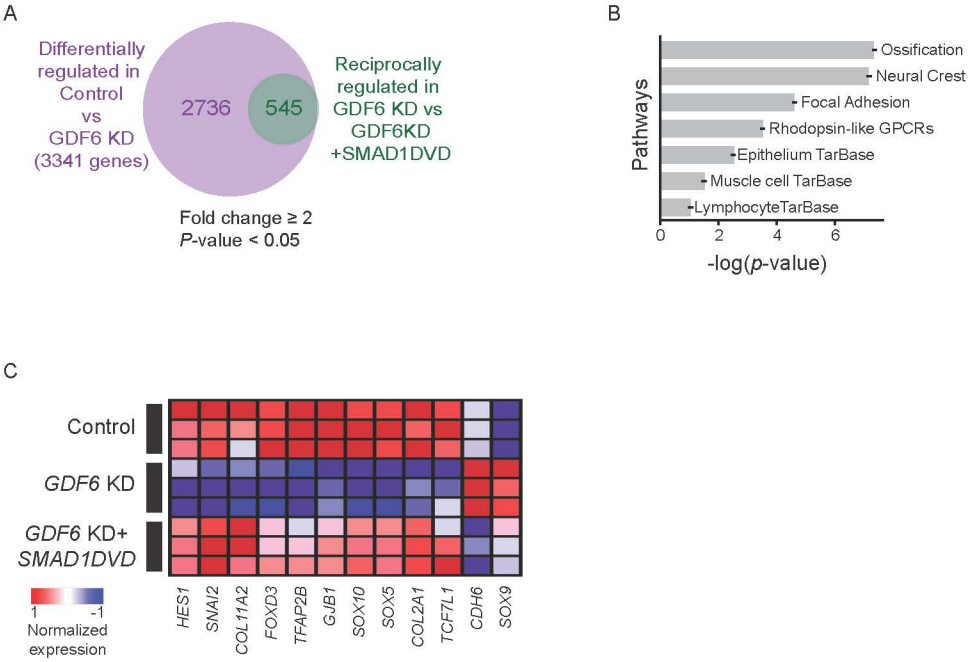

Figure 2
A) Genes differentially regulated upon GDF6 knockdown (purple circle) and genes reciprocally regulated in SMAD1DVD-expressing cells upon GDF6 knockdown (green circle). B) Pathway analysis with the 545 reciprocally regulated genes. C) Heat map of neural crest genes identified in pathway analysis.

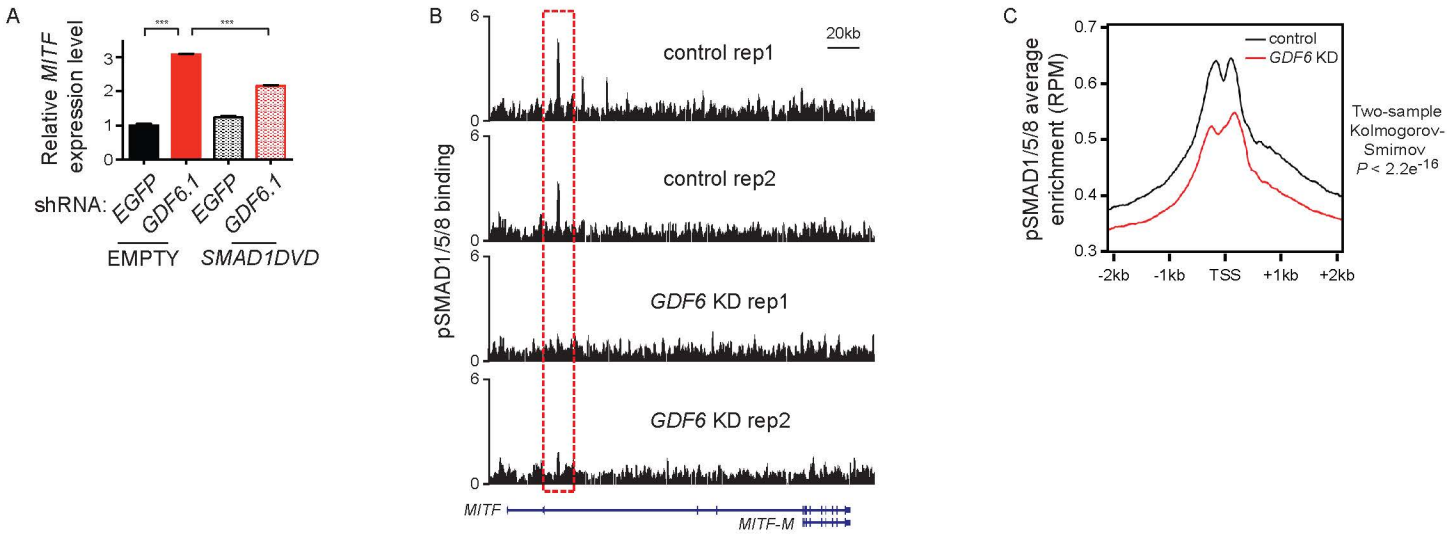

Figure 3

A) qRT-PCR of MITF (top) and TRP1 (bottom) in A375-empty or A375-SMAD1DVD cells with GDF6 knockdown. Left brackets, expression is upregulated upon GDF6 knockdown. Right brackets, expression is less upregulated in SMAD1DVD-expressing cells upon GDF6 knockdown. B) phospho-SMAD1/5/8 ChIPseq reads across the MITF locus in GDF6-knockdown A375 cells. C) Aggregation plot of phospho-SMAD1/5/8 ChIPseq binding at annotated TSSs in GDF6-knockdown A375 cells.

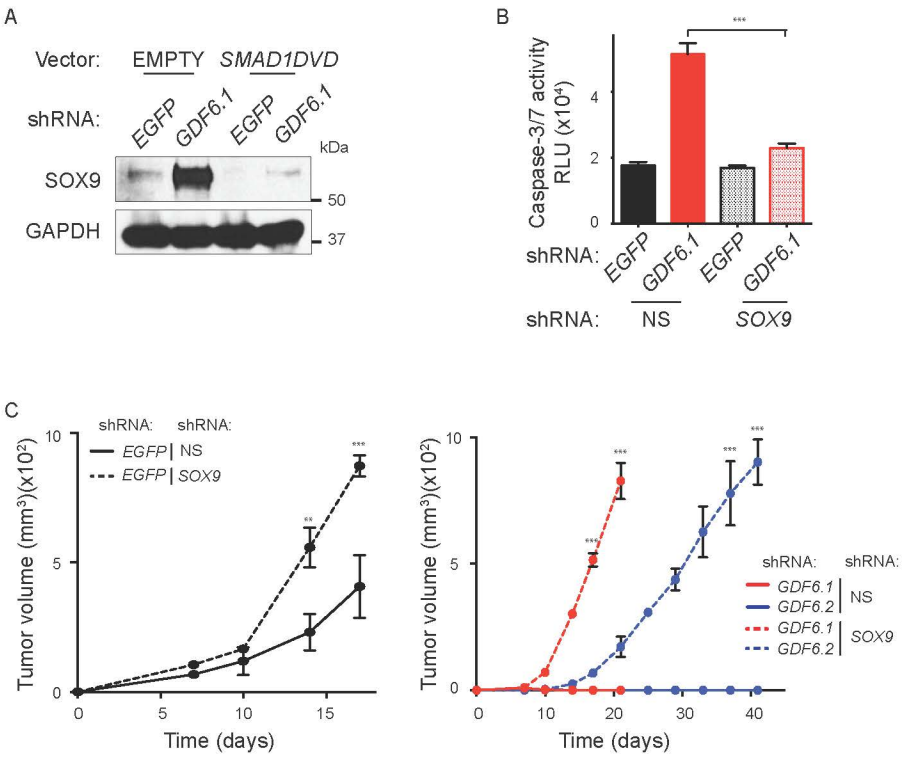

Figure 4
A) Immunoblots of SOX9 in A375-empty or A375-SMAD1DVD cells with GDF6 knockdown.
B) Caspase-3/7 activity in A375-non-silencing or A375-shSOX9 cells with GDF6 knockdown.
C) Mouse xenograft assay with A375-non-silencing or A375-shSOX9 cells expressing shEGFP (left) or GDF6-targeted shRNAs (right). Error bars indicate s.e.m.; n=3. Two-tailed Student's t-test, **P< 0.01, ***P< 0.001.

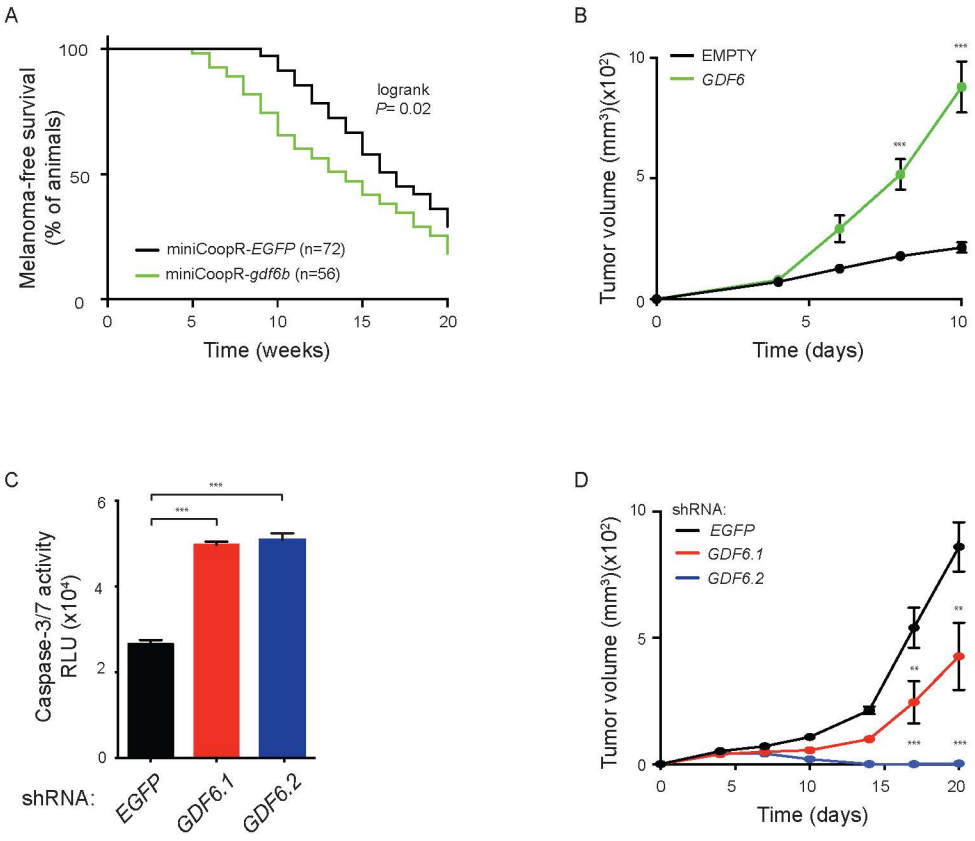

Figure 5

A) Melanoma-free survival curves for Tg(mitfa:BRAF(V600E));p53(lf);mitfa(lf) zebrafish injected with miniCoopR-gdf6b or miniCoopR-EGFP. B) Mouse xenograft assay with GDF6-overexpressing A375 cells. C) Caspase-3/7 activity measured as relative luciferase units (RLU) in A375 cells upon GDF6 knockdown. D) Mouse xenograft assay with GDF6-knockdown A375 cells. Error bars indicate s.e.m.; n=3. Two-tailed Student's t-test, **P< 0.01, ***P< 0.001.

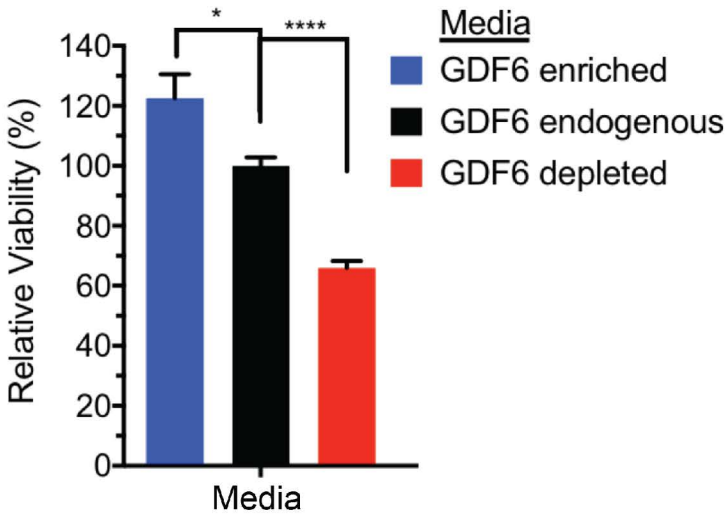

Figure 6
Addition of GDF6 enriched media rescues viability of A375 cells depleted of GDF6 by shRNA knockdown.

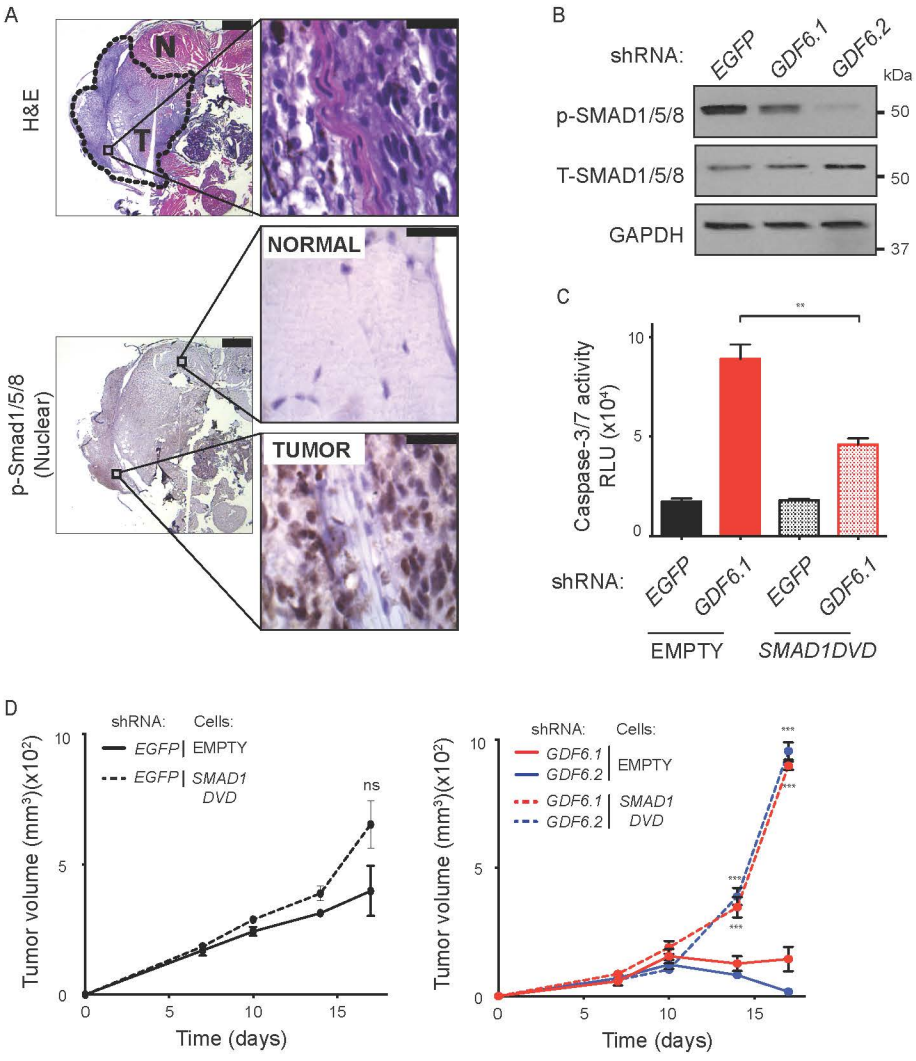

Figure 7

A) Stained transverse sections of a Tg(mitfa:BRAF(V600E));p53(lf) zebrafish bearing an invasive melanoma in the dorsal musculature. Left, scale bar, 500 µm. Right, scale bar, 50 µm. T, tumor. N, normal. B) Immunoblots of GDF6-knockdown A375 cells. C) Caspase-3/7 activity measured as relative luciferase units (RLU; caspase-glo assay) in A375-empty or A375-SMAD1DVD cells expressing shEGFP or shGDF6.1. D) Tumor formation in mice injected with A375-empty or A375-SMAD1DVD cells expressing shEGFP (left) or with GDF6 knockdown (right).

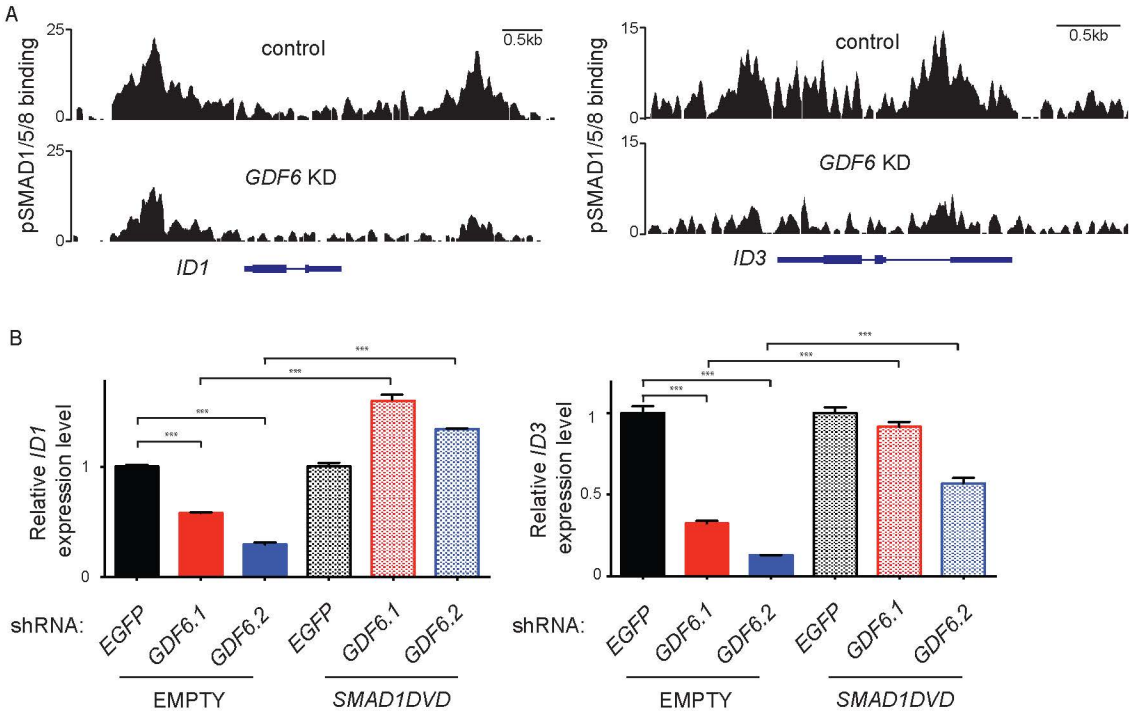

Figure 8
A) phospho-SMAD1/5/8 binding to the ID1 locus (left) and ID3 locus (right) in A375 melanoma cells expressing shEGFP or shGDF6.1. B) qRT-PCR showing expression of ID1 (left) and ID3 (right) in A375-empty or A375-SMAD1DVD cells expressing an shRNA targeting EGFP or two independent GDF6-targeted shRNAs. Left two brackets, ID gene expression is downregulated upon GDF6 knockdown. Right two brackets, downregulation of ID gene expression is reversed in SMAD1DVD-expressing cells upon GDF6 knockdown. Error bars indicate s.e.m.; n=3. Two-tailed Student's t-test, ***P< 0.001.

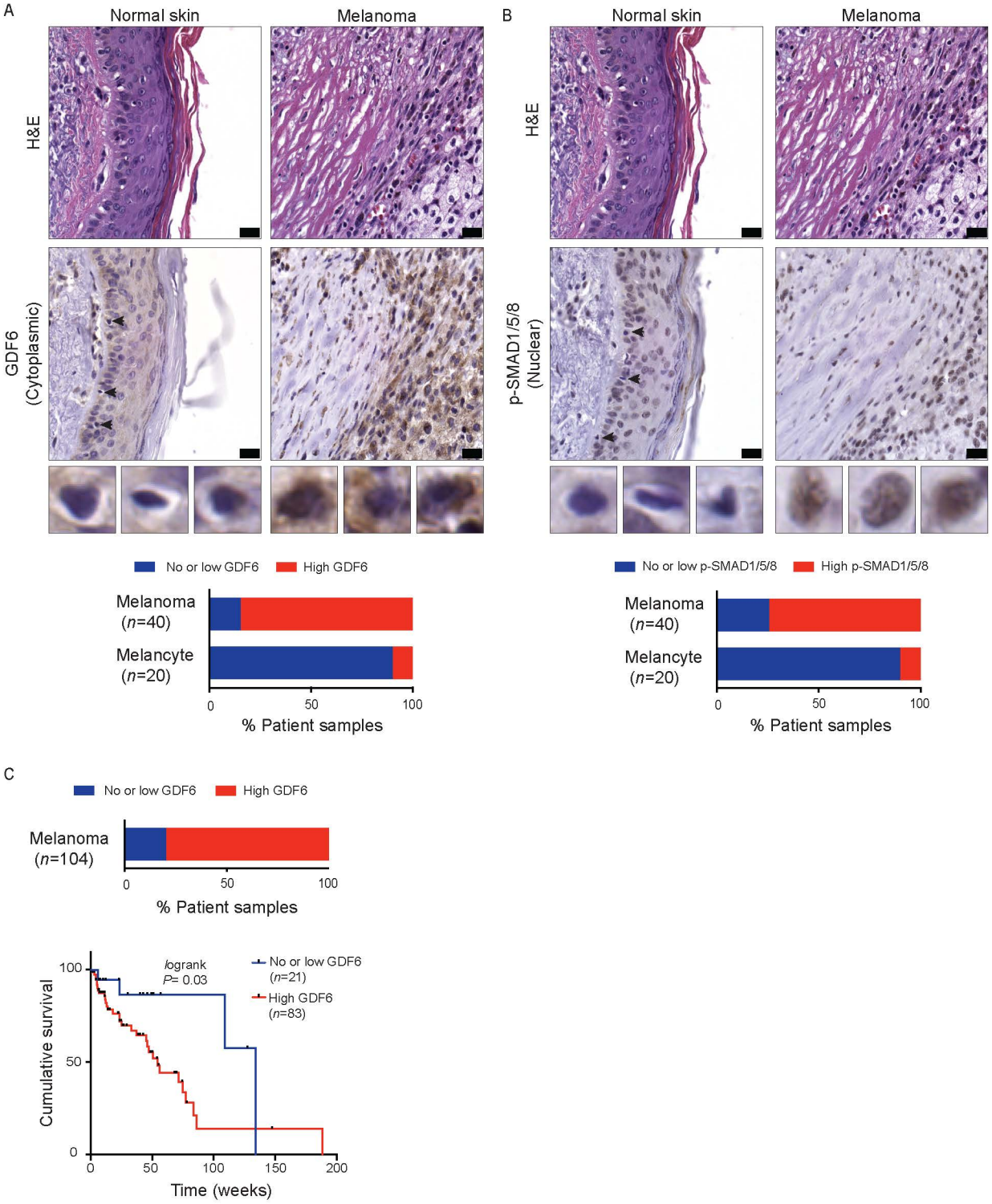

Figure 9

A) Stained human melanoma and adjacent skin samples. Melanocytes are indicated (arrowheads). Scale bar, 25µm. Individual cells are shown below. Bottom, quantification of samples based on GDF6 expression. B) phospho-SMAD1/5/8 immunostaining of the same sample cohort. C) Top, quantification of tissue microarray sample cohort based on GDF6 expression. Bottom, Kaplan-Meier analysis of patients with no or low versus high GDF6 expression.

CRAIG JOSEPH CEOL
Assistant Professor
Program in Molecular Medicine and Department of Molecular, Cell and Cancer Biology,
University of Massachusetts Medical School
Albert Sherman Center, AS6.1041, 368 Plantation Street, Worcester, MA 01605
Date prepared: September 30, 2016

EDUCATION

Yale University, New Haven, CT — 1989-1993
B.S./M.S. combined degree in Molecular Biophysics and Biochemistry
Research Advisor: Dr. Lynne Regan

Massachusetts Institute of Technology, Cambridge, MA — 1995-2003
Ph.D. degree in Biology
Research Advisor: Dr. H. Robert Horvitz

Massachusetts Institute of Technology, Cambridge, MA — 2003-2004
Postdoctoral Fellow, Department of Biology, HHMI
Research Advisor: Dr. H. Robert Horvitz

Harvard Medical School, Children's Hospital Boston, Boston, MA — 2004-2008
Postdoctoral Fellow, Division of Hematology/Oncology, HHMI
Research Advisor: Dr. Leonard I. Zon

PROFESSIONAL EXPERIENCE

Research Associate, Eli Lilly and Company — 1993-1995
Division of Bioproduct Development

Instructor, Harvard Medical School, Children's Hospital Boston, — 2008-2009
Division of Hematology/Oncology

Assistant Professor, University of Massachusetts Medical School — 2010-
Program in Molecular Medicine and Program in Cell Dynamics
Department of Cancer Biology

HONORS AND AWARDS

Yale University:
B.S./M.S. four-year degree, Molecular Biophysics and Biochemistry — 1991-1993
Yale University Summer Study Grant — 1991
Distinction in Molecular Biophysics and Biochemistry — 1993

Massachusetts Institute of Technology:
Koch Predoctoral Research Fellow — 1999-2000

Children's Hospital Boston and Harvard Medical School:
Damon Runyon Cancer Research Foundation Postdoctoral Fellowship — 2005-2007
American Cancer Society Postdoctoral Fellowship (declined) — 2005
Winner, Poster prize, Keystone Symposium, Santa Fe, NM — 2006
Advances in the Understanding and Treatment of Melanoma
Winner, Presentation prize, Harvard Stem Cell Institute Symposium — 2008
Charles A. King Trust of The Medical Foundation Postdoctoral Fellowship — 2008-2009

NIH Pathway to Independence Award (K99/R00), NIAMS 2009-2013

University of Massachusetts Medical School:

Worcester Foundation for Biomedical Research Award 2011-2012
American Cancer Society Research Scholar Award 2012-2016
Kimmel Scholar Award 2013-2015
Department of Defense Cancer Career Development Award 2013-2015

FUNDING

Active:

RSG-12-150-01-DDC Research Scholar Award, American Cancer Society, Ceol (PI)
Epigenetic determinants of melanoma initiation and maintenance.

R01AR063850 NIH/NIAMS, Ceol (PI)
Use of comparative oncogenomics to identify novel regulators of melanoma progression.

UL1TR000161 UMMS NHMPP Award, Ceol & Yang (PIs)
GDF-6 blocking antibodies as cancer therapeutics.

Concluded:

CA120099 Dept of Defense Peer Reviewed Cancer Career Development Award, Ceol (PI)
Uncovering the role of BMP signaling in melanocyte development and melanoma tumorigenesis.

SKF-13-123 Kimmel Scholar Award, Ceol (PI)
Mechanisms underlying melanoma initiation and maintenance.

R00AR056899 Pathway to Independence Award, NIH/NIAMS, Ceol (PI)
Identifying events and genetic regulators of melanoma progression

P60016170000122 Worcester Foundation for Biomedical Research, Ceol (PI)
Use of comparative genomics to identify oncogenes.

Scientific Meeting Grant, The Company of Biologists, Ceol (PI)
Zebrafish Disease Models 7 conference, Madison, WI, June 28-July 1, 2014

TEACHING AND MENTORING

Teaching:

M.D./Ph.D. Research Tutorial, one discussion group (3hr). 2010
Ph.D. Summer RAPS (Reading, Analysis, Problem Solving paper review), one discussion group (2hr). 2010
Cancer Biology, one lecture (2hr), one discussion group (2hr). 2010-
Molecular Biology of the Cell Cycle, one lecture (0.5hr), one discussion group (2hr) 2011, 2015
Stem Cell and Regenerative Biology. Co-coordinator, two lectures and discussion groups (4hr) plus organizational responsibilities. 2011-2012
RAPS, Block II (2hr). 2011-
Topics in Molecular Medicine, one lecture and discussion group (2hr). 2012
MDP740 Developing solutions to research problems, lecture and discussion (2hr) 2014
GSBS Foundations Course. Cancer and Cell Signaling module. Co-coordinator, nine discussion groups (18hrs) plus organizational responsibilities 2016-

Advisory and supervisory responsibilities:

Name	Position	Year(s)
Rajesh Vyas	Postdoctoral Fellow	2014-

Ana Neto	Postdoctoral Fellow	2011-	NRSA Fellow, NCI
Fang Liu	Postdoctoral Fellow	2013	
Corrie Painter	Postdoctoral Fellow	2012-4	CRI Irvington Inst. Fellow
Sharanya Iyengar	Graduate Student	2010-	
James Neiswender	Graduate Student	2010-	
Arvind Venkatesan	Graduate Student	2011-	
Revati Darp	Graduate Student	2014-	
Alec Gramann	MD/PhD Student	2015-	TL1 Trainee, NCATS
Tyler Frantz	MD/PhD Student	2015-	T32 Trainee, NCI
Eli Freiman	Medical Student	2012	
Alysia Bryll	Rotating MD/PhD Student	2015	
Ciearra Smith	Rotating Graduate Student	2014	
Heather Kolpa	Rotating Graduate Student	2010	
Jennifer Maurer	Rotating Graduate Student	2010	
James Ritch	Rotating Graduate Student	2010	
Lin Lin	Rotating Graduate Student	2010	
Tadas Buivydas	Undergrad. Student (Worcester St. University)	2016	
Sukanya Murali	Undergrad. Student (Anna University – Chennai)	2013	
Brittney Logan	Undergrad. student (W. New England University)	2013	
Justin Peter Hess	Undergrad. Student (WPI)	2012	

Dissertation committees:
Shawna Guillemette, UMass Medical School, Cancer Biology Program
Tomoko Tabuchi, UMass Medical School, Interdisciplinary Graduate Program
David Driscoll, UMass Medical School, Cancer Biology Program
Anna Malinkevich, UMass Medical School, Interdisciplinary Graduate Program
Cheng Chang, UMass Medical School, Cancer Biology Program (Chair)
Nomeda Girnius, UMass Medical School, Cancer Biology Program
Lin Lin, UMass Medical School, Cancer Biology Program (Chair)
James Ritch, UMass Medical School, Interdisciplinary Graduate Program
Nicola Kearns, UMass Medical School, Interdisciplinary Graduate Program
Neha Diwanji, UMass Medical School, Cancer Biology Program
Nicholas Panzarino, UMass Medical School, Cancer Biology Program (Chair)
Zeynep Itah, UMass Medical School, Cancer Biology Program

Qualifying examination committees:
Christopher Clark, UMass Medical School, Neuroscience Program
Caitlin Fogarty, UMass Medical School, MD/PhD Program
Nomeda Girnius, UMass Medical School, Interdisciplinary Graduate Program
Chien-Min Hung, UMass Medical School, Interdisciplinary Graduate Program
James Ritch, UMass Medical School, Interdisciplinary Graduate Program
Lin Lin, UMass Medical School, Cancer Biology Program (Chair)
Ly-She Ee, UMass Medical School, Interdisciplinary Graduate Program
Shubham Dutta, UMass Medical School, Interdisciplinary Graduate Program
Nicola Kearns, UMass Medical School, Interdisciplinary Graduate Program
Hsi-Ju Chen, UMass Medical School, Interdisciplinary Graduate Program
Nicholas Panzarino, UMass Medical School, Cancer Biology Program (Chair)

Peter Cruz-Gordillo, UMass Medical School, Medical Scientist Training Program

SERVICE

University of Massachusetts Medical School and local:

Sherman Center Labs NTI/GTC/CVC/Diabetes Focus Group	2010
Diabetes and Endocrinology Research Center (grant reviewer, ad hoc)	2011
AP Biology High School Outreach Program (host)	2011-
University of Massachusetts Medical School Convocation (Dinner and Dialogue event speaker and panelist)	2011
University of Massachusetts Medical School visit of Young President's Organization & World President's Organization (speaker)	2011
University of Massachusetts Medical School Development Council meeting (speaker)	2012
University of Massachusetts Medical School BARG Organization (speaker)	2012
LCME accreditation of University of Massachusetts Medical School (Junior Faculty cohort)	2012
University of Massachusetts Chancellor's Review (Faculty Review Committee)	2012
Wachusett High School Science Seminar	2012
University of Massachusetts Medical School Science to Trades Seminar	2013
WSRS interview w/ Greg Byrne in support of UMMS Cancer Walk	2013
UMMS Development Office – lab tours with donor groups	2013-
MassAHEC Network Frontiers in Science Seminar	2014
NIH BEST Award Focus Group	2014
Hudson Hoagland Society annual meeting (speaker)	2014
WSRS interview W/ Jordan Levy in support of UMMS Cancer Walk	2014
University of Massachusetts Medical School Media Day (speaker)	2014-
UMMS Communications Office – 'Here for a Reason' campaign	2014
Research Roundtable, UMASS President Meehan visit	2015
Research Roundtable, UMASS Morningside Group visit	2015
Panelist, Cancer Walk Kickoff Breakfast	2016

Referee for journals:

Molecular and Cellular Oncology – Peer Review Board 2014-
PLoS Genetics – ad hoc 2009-
Proceedings of the National Academy of Sciences USA – ad hoc 2009-
Molecular and Cellular Biology – ad hoc 2010-
PLoS Biology – ad hoc 2011-
FASEB Journal – ad hoc 2012-
Experimental Cell Research – ad hoc 2012-
Genome Research – ad hoc 2012-
Journal of Investigative Dermatology – ad hoc 2012-
Journal of Visualized Experiments – ad hoc 2013-
Cell Death and Differentiation – ad hoc 2013-
Disease Models and Mechanisms – ad hoc 2013-
Cell Death and Disease – ad hoc 2014-
Developmental Cell – ad hoc 2016-
eLife – ad hoc 2016-

Grant review and study section service:

Children's Tumor Foundation Research Grant Review Panel (CTF-RGRP) - 2013-

National Centre for the Replacement, Refinement and Reduction of Animals in Research (Ad Hoc Reviewer) - 2010
University of Massachusetts Medical School Diabetes and Endocrinology Research Center (Ad Hoc Reviewer) - 2010
Association for International Cancer Research (Ad Hoc Reviewer) - 2011
NIH, Cancer Genetics Study Section (CG) (Ad Hoc Reviewer) - 2012
Medical Research Council (United Kingdom) (Ad Hoc Reviewer) - 2013, 2015
NIH, Genes, Genomes and Genetics Special Emphasis Review panel ZRG1 GGG-E - 2015
MSKCC-CCNY U54 Translational Research (Ad Hoc reviewer) - 2015

Society memberships:
Society for Melanoma Research, 2009-
American Society for Cell Biology, 2012-
American Association for Cancer Research, 2012-
Zebrafish Disease Models Society, 2014-
Pan-American Society for Pigment Cell Research, 2014-

Meetings and community service:
Co-organizer, Zebrafish Disease Models 7, Madison, WI, 2014
Co-chair, Cancer Working Group, Zebrafish Disease Models Society, 2014-
Session Chair, Society for Developmental Biology Northeast meeting, Woods Hole, MA, 2015
Abstract reviewer, Society of Investigative Dermatology Annual Meeting, Scottsdale, AZ, 2016
Abstract reviewer, Zebrafish Disease Model 9, Singapore, 2016

PUBLICATIONS

Original reports:

1. **Ceol, C.J.** and Horvitz, H.R. (2001). *dpl-1* DP and *efl-1* E2F act with *lin-35* Rb to antagonize Ras signaling in *C. elegans* vulval development. Mol. Cell. *7*, 461-73.
   ‡ This paper is highlighted by the Faculty of 1000.
2. Thomas, J.H.*, **Ceol, C.J.***, Schwartz, H.T. and Horvitz, H.R. (2003). New genes that interact with *lin-35* Rb to negatively regulate the *let-60 ras* pathway in *Caenorhabditis elegans*. Genetics. *164*, 135-51.
3. **Ceol, C.J.** and Horvitz, H.R. (2004). A new class of *C. elegans* synMuv genes implicates a Tip60/NuA4-like HAT complex as a negative regulator of Ras signaling. Dev. Cell. *6*, 563-76.
   ‡ This paper is highlighted by the Faculty of 1000.
4. **Ceol, C.J.**, Stegmeier, F., Harrison, M.M. and Horvitz, H.R. (2006). Identification and classification of genes that act antagonistically to *let-60* Ras signaling in *Caenorhabditis elegans* vulval development. Genetics. *173*, 709-26.
5. Harrison, M.M., **Ceol, C.J.**, Lu X. and Horvitz, H.R. (2006). Some *C. elegans* class B synthetic multivulva proteins encode a conserved LIN-35 Rb-containing complex distinct from a NuRD-like complex. Proc. Natl. Acad. Sci. USA. *103*, 16782-7.
6. White, R.M., Sessa, A., Burke, C., Bowman, T., LeBlanc, J., **Ceol, C.J.**, Bourque, C., Dovey, M., Goessling, W., Burns, C.E. and Zon. L.I. (2008). Transparent adult zebrafish as a tool for in vivo transplantation analysis. Cell Stem Cell, *2*, 183-9.
7. Langenau, D.M., Keefe, M.D., Storer, N.Y., Jette, C.A., Smith, A.C., **Ceol, C.J.**, Bourque, C., Look, A.T. and Zon, L.I. (2008). Coinjection strategies to modify radiation sensitivity and tumor initiation in transgenic zebrafish, Oncogene, *27*, 4242-8.

8. Goessling, W., North, T.E., Lord, A.M., **Ceol, C.J.**, Weidinger, G., Lee, S., Strijbosch, R., Haramis, A., Puder, M., Clevers, H., Moon, R.T. and Zon, L.I. (2008). APC mutant zebrafish uncover a changing temporal requirement for wnt signaling in liver development. *Dev. Biol.*, *320*, 161-74.
9. Freeman, J.L., **Ceol, C.J.**, Feng, H., Langenau, D.M., Belair, C., Stern, H.M., Song, A, Paw, B.H., Look, A.T., Zhou, Y., Zon, L.I. and Lee, C. (2009). Construction and application of a cytogenetically-validated zebrafish-specific array CGH platform. *Genes Chromosomes Cancer*, *48*, 155-70.
10. North, T.E., Goessling, W., Peeters, M., Li, P., **Ceol, C.J.**, Lord, A.M., Weber, G.J., Harris, J., Cutting, C.C., Huang, P., Dzierzak, E., Zon, L.I. (2009). Hematopoetic stem cell development is dependent on blood flow. *Cell*, *137*, 436-48.
11. **Ceol, C.J.***, Houvras, Y.*, Jane-Valbuena, J., Bilodeau, S., Orlando, D., Battisti, V., Fritsch, L., Lin, W., Hollmann, T.J., Ferré, F., Bourque, C., Burke, C., Turner, L., Uong, A., Johnson, L.A., Beroukhim, R., Mermel, C., Loda, M., Ait-Si-Ali, S., Garraway, L., Young R.A. and Zon, L.I. (2011). The *SETDB1* histone methyltransferase is recurrently amplified in and accelerates melanoma. *Nature*, *471*, 513-7.
12. Richardson, J., Zeng, Z., **Ceol, C.J.**, Jackson, I.J., Patton, E.E. (2011). *BRAF^{V600E}* nevi regenerate from an undifferentiated precursor population in zebrafish. *Pigment Cell Melanoma Research*, *24*, 378-81.
13. Lian, C.G., Xu. Y., **Ceol, C.J.**, Wu, F., Larson, A., Dresser, K., Xu, W., Tan, L., Zhan, Q., Lee, C., Hu, D., Lian, B.Q., Kleffel, S., Yang, Y., Khorasani, A.J., Lezcano, C., Duncan, L.M., Scolyer, R.A., Thompson, J.F., Kakavand, H., Houvras, Y., Zon, L., Mihm Jr., M.C., Kaiser, U.B., Schatton, T., Woda, B.A., Murphy, G.F. and Shi, Y.G. (2012). Loss of 5-hydroxymethylcytosine is an epigenetic hallmark of melanoma. *Cell*, *150*, *1135-46*.
‡ This paper is highlighted by the Faculty of 1000.
14. Iyengar, S., Houvras, Y. and **Ceol, C.J.** (2012). Screening for melanoma modifiers using a zebrafish autochthonous tumor model. *Journal of Visualized Experiments*, *69, e50086*.
15. Painter, C.A. and **Ceol, C.J.** (2014). Zebrafish as a platform to study tumor progression. *Methods in Molecular Biology*, *1176, 143-55*.
16. Iyengar, S., Kasheta, M. and **Ceol, C.J.** (2015). Poised regeneration of zebrafish melanocytes involves direct differentiation and concurrent replenishment of tissue-resident progenitor cells. *Developmental Cell*, *33*, *631-43*.
‡ Previewed in Kang, J., Karra, R. and Poss, K. (2015) Back in black. *Developmental Cell*, *33*, *623-4*.
17. Wojciechowska, S., van Rooijen, E., **Ceol, C.**, Patton, E.E. and White, R. (2016). Generation and analysis of zebrafish melanoma models. *Methods in Cell Biology*, in the press.
18. Moore, F.E., Garcia, E.G., Lobbardi, R., Jain, E., Tang, Q., Moore, J.C., Cortes, M., Molodtsov, A., Kasheta, M., Luo, C.C., Garcia, A.J., Mylvaganam, R., Yoder, J.A., Blackburn, J.S., Sadreyev, R.I., **Ceol, C.J.**, North, T.E. and Langenau, D.M. (2016). Single-cell transcriptional analysis of normal, aberrant and malignant hematopoiesis in zebrafish. *Journal of Experimental Medicine*, in the press.
19. Wojciechowska, S., Zeng, Z., Lister, J.A., **Ceol, C.J.**, Patton, E.E. (2016). Melanoma regression and recurrence in zebrafish. *Methods Molecular Biology*, in the press.
20. Venkatesan, A.M., Vyas, R., Dresser, K., Gujja, S., Bhatnagar, S., Chhangawala, S., Gomes, C., Xi, H.S., Lian, C.G., Houvras, Y., Edwards, Y.J.K., Deng, A., Green, M. and **Ceol, C.J.** (2016). GDF6 ligand-induced BMP signaling induces a neural crest identity and is critical for survival and growth of melanomas. Submitted.

Reviews and commentary:

1. **Ceol, C.J.**, Pellman D. and Zon, L.I. (2007). APC and colon cancer: two hits for one. *Nat. Med*. *13*, 1286-7.
2. **Ceol, C.J.***, Houvras, Y.*, White R.M.* and Zon, L.I. (2008). Melanoma biology and the promise of zebrafish. *Zebrafish* *5*, 247-55.
3. **Ceol, C.J.** (2011). Acta Eruditorum: Certain genes accelerate melanoma development. *Dermatology World* *21*, 11-12.
4. **Ceol, C.J.** and Houvras, Y. (2016). Uncharted waters: zebrafish cancer models navigate a course of discovery. *Advances in Experimental Medicine and Biology, Cancer and Zebrafish: Mechanisms, Techniques and Models*, *916*, 3-19.

Cover art:

1. **Ceol, C.J.***, Houvras, Y.*, Jane-Valbuena, J., Bilodeau, S., Orlando, D., Battisti, V., Fritsch, L., Lin, W., Hollmann, T.J., Ferré, F., Bourque, C., Burke, C., Turner, L., Uong, A., Johnson, L.A., Beroukhim, R., Mermel, C., Loda, M., Ait-Si-Ali, S., Garraway, L., Young R.A. and Zon, L.I. (2011). The *SETDB1* histone methyltransferase is recurrently amplified in and accelerates melanoma. *Nature*, *471*, 513-7.
2. Iyengar, S., Kasheta, M. and **Ceol, C.J.** (2015). Poised regeneration of zebrafish melanocytes involves direct differentiation and concurrent replenishment of tissue-resident progenitor cells. *Developmental Cell*, *33*, 631-43.

ORAL PRESENTATIONS

Meeting presentations:

East Coast *C. elegans* Meeting, Boston, MA	1998
International *C. elegans* Meeting, Madison, WI	1999
East Coast *C. elegans* Meeting, Durham, NH	2002
Keystone Symposium, *Advances in the Understanding and Treatment of Melanoma*, Santa Fe, NM	2006
Gordon Conference, *Cancer Models and Mechanisms*, Les Diablerets, Switzerland	2008
8th International Conference on Zebrafish Development and Genetics, Madison, WI	2008
Harvard Stem Cell Institute Research Symposium, Boston, MA	2008
9th International Conference on Zebrafish Development and Genetics, Madison, WI	2009
3rd Zebrafish Disease Models Conference, Boston, MA	2010
Connecticut Valley Zebrafish Meeting, Middletown, CT	2010
Gordon Conference, *Cancer Genetics and Epigenetics*, Ventura, CA	2011
Biotechcellence 2012 National Technical Symposium Anna University, Chennai, India (via videoconference)	2012
10th International Conference on Zebrafish Development and Genetics, Madison, WI (workshop co-coordinator)	2012
International Federation of Pigment Cell Societies, Pigment Cell Development Workshop, Edinburgh, UK	2013
5th European Melanoma Conference, *Basic and clinical research join forces to defeat melanoma*, Marseille, France	2013
6th Zebrafish Disease Models Conference, Murcia, Spain	2013
7th Zebrafish Disease Models Conference, Madison, Wisconsin (in place of maternity leave postdoc Ana Neto)	2014
22nd International Pigment Cell Conference, *Bringing colours to life*, Singapore	2014

52nd Annual Meeting of The American Society of Dermatopathology, San Francisco, CA 2015
PanAmerican Society for Pigment Cell Research Conference, Irvine, CA 2015
The Allied Genetics Conference, Orlando, FL 2016
PanAmerican Society for Pigment Cell Research Conference, Baltimore, MD 2016
8th Aquatic Animal Models of Human Disease Conference, Birmingham, AL 2017

Invited seminar presentations:

Hubrecht Institute, Utrecht, Netherlands 2008
Cancer Genomics and Developmental Biology Programme Seminar

Whitehead Institute, Massachusetts Institute of Technology, Cambridge, MA 2008
Whitehead Seminar Series for High School Teachers: Contolling Genes

Providence College, Providence, RI 2011
Biology Department Seminar

UMass Medical School, Worcester, MA 2011
Cutaneous Tumor Board, Pathology Department

University of Rochester Medical Center, Rochester, NY 2011
Biomedical Genetics Department Seminar

Quinsigamond Dermatological Society, Worcester, MA 2011
Grand Rounds

Carnegie Institution, Baltimore, MD 2012
Department of Embryology Seminar

National Institutes of Health, Bethesda, MD 2012
NIH Comparative Biomedical Scientist Program Symposium

University of Massachusetts Medical School, Worcester, MA 2012
Cancer Biology Retreat

Assumption College, Worcester, MA 2012
Seminar in Life Sciences

University of Massachusetts Medical School, Worcester, MA 2013
Microbiology and Physiological Systems Department Seminar

Tufts University School of Medicine, Boston, MA 2013
Molecular Physiology and Pharmacology Retreat (Keynote)

Centro Andaluz de Biología del Desarrollo, Seville, Spain 2013
CABD Institute Seminar

University of Michigan, Ann Arbor, MI 2014
Molecular, Cellular and Developmental Biology Seminar

University of Massachusetts, Dartmouth, MA 2014
Biology and Bioengineering Seminar

Tufts University, Medford, MA 2015
American Cancer Society Relay for Life Seminar

University of Massachusetts Medical School, Worcester, MA 2015
Division of Hematology/Oncology Grand Rounds

MassBiologics, Boston, MA 2016
MassBiologics Research Seminar

Yale University, New Haven, CT 2016
Internal Medicine Seminar Series

Ligand-dependent BMP signaling reawakens an embryonic neural crest identity to promote melanoma

Authors:

Arvind M. Venkatesan[1,2], Rajesh Vyas[1,2], Alec K. Gramann[1,2], Karen Dresser[3], Sharvari Gujja[1], Sanchita Bhatnagar[1,2,4†], Sagar Chhangawala[5], Camilla Borges Ferreira Gomes[6], Hualin Simon Xi[1†], Christine G. Lian[6], Yariv Houvras[5], Yvonne J. K. Edwards[1], April Deng[3], Michael Green[1,2,4] & Craig J. Ceol[1,2]*

Affiliations:

1 Program in Molecular Medicine, University of Massachusetts Medical School, Worcester Massachusetts 02115, USA

2 Department of Molecular, Cell and Cancer Biology, University of Massachusetts Medical School, Worcester Massachusetts 02115, USA

3 Department of Pathology, University of Massachusetts Medical School, Worcester Massachusetts 02115, USA

4 Howard Hughes Medical Institute, University of Massachusetts Medical School, Worcester Massachusetts 02115, USA

5 Departments of Surgery and Medicine, Weill Cornell Medical College, New York New York 10065, USA

6 Program in Dermatopathology, Department of Pathology, Brigham and Women's Hospital, Harvard Medical School, Boston Massachusetts 02115, USA

*Corresponding author, email [Craig.Ceol@umassmed.edu]

† Present addresses: Departments of Biochemistry and Molecular Genetics, University of Virginia School of Medicine, Charlottesville, Virginia 22903, USA (S.B.); Computational Sciences Center of Emphasis, Pfizer Worldwide Research & Development, Cambridge Massachusetts 02139, USA (H.S.X.)

Abstract:

Certain cancer-associated genetic changes are postulated to be programmatic in nature – they modify the identity of a nascent cancer cell thereby impacting multiple cellular processes to promote cancer progression. Melanomas adopt a neural crest identity, but the importance and mechanism of adopting such an identity are poorly understood. Through comparative oncogenomics of human and zebrafish melanomas, we identified a BMP ligand, *GDF6*, which reawakens neural crest features in melanoma cells, allowing them to remain undifferentiated and survive. Our study uncovers reiteration of ligand-dependent developmental signaling as a means to fundamentally alter cancer cell identity. Targeting *GDF6* and other ligands can be achieved through conventional approaches, providing new avenues for cancer therapy.

Main Text:

Phenotypic hallmarks of cancer cells can be gained through a succession of genetic changes that affect cancer-relevant processes such as cell proliferation or cell death. However, certain genetic alterations, on their own, can be programmatic in nature, enabling a cell to gain several pro-tumorigenic activities simultaneously. Such an event has been proposed for melanomas, which adopt a neural crest identity even at the earliest stages of tumorigenesis (*1*). However, the means of adopting this identity and the cellular processes affected by it are unknown. As described below, through functional genomic analyses we have uncovered an embryonic signaling system that is used in melanomas to govern cell identity and tumorigenesis.

We began our study by attempting to deconstruct the complex profile of copy number variation (CNV) in the melanoma genome. A major challenge in the field of cancer genomics has been to distinguish, from a chromosomal segment subject to CNV, tumor-promoting driver genes from large numbers of uninvolved passenger genes. To address this challenge we used comparative oncogenomics between human and zebrafish melanomas, because the genomic reorganization that has occurred over time is predicted to place orthologous driver genes next to different neighboring passenger genes in each species. We defined CNVs in melanomas from a *Tg(mitfa:BRAFV600E); p53(lf)* zebrafish strain (*2*) (Fig. 1A; Table S1). Genes from recurrently amplified intervals were compared to their human orthologs (*3, 4*). The degree of overlap between orthologs amplified in both species is greater than would be expected by chance (Fig. 1B; Table S2), suggesting that amplification of similar driver genes mechanistically underlies tumor formation in both species. To further winnow the list of candidates, we analyzed transcriptional profiles of zebrafish melanomas and normal melanocytes and identified *gdf6b,* an ortholog of the BMP factor *GDF6*. In addition to being recurrently amplified, *gdf6b* mRNA and

protein were upregulated in zebrafish melanomas (Fig. 1C,D; Fig. S1A,B; Fig. S2). The second zebrafish ortholog of human *GDF6*, *gdf6a*, although not amplified, was among the most transcriptionally upregulated genes in melanomas. Along with being recurrently amplified, human *GDF6* was also transcriptionally upregulated in melanomas (Fig. S1C). Expression of *GDF6* orthologs in melanomas was interesting as normal expression of these genes is limited to embryonic tissues.

We next assessed how a gain or loss of *GDF6* affected melanoma progression. In zebrafish, *gdf6b* expression in the melanocyte lineage accelerated melanoma onset as compared to controls (Fig. 1E). Accelerated onset was dependent on *BRAFV600E* and loss of *p53,* as expression of *gdf6b* in *Tg(mitfa:BRAFV600E)* transgene (n=33) or *p53(lf)* (n=24) backgrounds alone did not produce tumors. In human melanoma cells, *GDF6* overexpression improved growth of cells *in vitro* and of xenografts, whereas *GDF6* knockdown had the opposite effect (Fig. 1F,G; Fig. S3A-H). Collectively these data indicate that *GDF6* acts as an oncogene via elevated expression. Acceleration of melanoma onset in zebrafish support a role in tumor initiation, and the ability of *GDF6* to facilitate growth and tumorigenic potential of melanoma cells suggests a further role in melanoma maintenance.

Encoding BMP ligands, *GDF6* genes are predicted to act through *SMAD1/5/8* transcription factors. Indeed, we found robust phospho-SMAD1/5/8 nuclear staining in zebrafish melanomas (Fig. 2A). Furthermore, transcriptome analyses of these melanomas indicated: a) robust upregulation of genes that support BMP signaling (Fig. S4A) and b) that *GDF6* orthologs were the only BMP ligands upregulated (Figure S4B). In human melanoma cells, *GDF6* modulation positively regulated phospho-SMAD1/5/8 levels (Fig. 2B; Fig. S5A). *GDF6* knockdown also reduced phospho-SMAD1/5/8 binding genome-wide (Fig. 2C; Fig. S5B).

Reduced binding to canonical BMP targets *ID1* and *ID3* was associated with a drop in their transcript levels (Fig. S5C,D). Inhibition of BMP signaling, either by *SMAD1* knockdown or the use of the small-molecule inhibitor DMH1, impaired growth of melanoma cells *in vitro* and of xenografts, similar to *GDF6* knockdown (Fig. S6A-H). In epistasis analyses, *GDF6* knockdown or DMH1 treatment had less impact on melanoma cells expressing an activated, phosphomimetic variant of *SMAD1*, *SMAD1DVD* (*5*) (Fig. 2D; Fig. S5D & S7). Together these data indicate that *GDF6* acts, at least in part, through *SMAD1* and therefore, the SMAD1/5/8 axis in promoting melanoma growth.

Since *GDF6* and *SMAD1* promote tumorigenesis, we sought to identify genes that were commonly regulated by both. Based on our genetic epistasis results, we predicted that expression of important genes would change upon *GDF6* knockdown but such changes would be reversed when *GDF6* knockdown was rescued by *SMAD1DVD*. We used RNAseq to define this set of reciprocally regulated genes (Fig. 2E; Table S3), and pathway analysis showed enrichment of genes defining ossification and neural crest pathways (Fig. 2F). Melanocytes initially develop from the embryonic neural crest. Several genes regulated by *GDF6* and *SMAD1DVD – SOX10, SOX9, TFAP2B, FOXD3, SNAI2* - are neural crest 'specifiers', genes that are initially expressed broadly in the neural crest and help to maintain neural crest identity (Fig. 2G) (*6*). As development proceeds, *SOX10* and *SOX9* expression becomes restricted to trunk and cranial neural crest, respectively. Since *GDF6* and *SMAD1DVD* upregulate *SOX10* and downregulate *SOX9,* the pattern of gene regulation most closely resembles trunk neural crest tissue that gives rise to melanocytes and other non-mesenchymal cells. Adopting a neural crest-like identity can contribute to the aggressive nature of melanoma cells (*7, 8*), and we hypothesized that *GDF6* promotes a trunk neural crest identity to facilitate melanoma initiation and progression.

To examine this hypothesis mechanistically, we focused on transcriptional targets of BMP signaling. ChIPseq data suggested that *GDF6* activates SMAD1/5/8 to directly regulate *MITF,* a key regulator of melanocyte development during embryogenesis (Fig. 2H). In control melanoma cells, phospho-SMAD1/5/8 bound to the *MITF* locus, and this binding was reduced in *GDF6* knockdown cells. Loss of phospho-SMAD1/5/8 binding was accompanied by upregulation of *MITF* and its target, the melanin biosynthesis gene *TRP1* (Fig. 2I). Upregulation of *MITF* and *TRP1* was less pronounced when *GDF6* knockdown was performed in *SMAD1DVD*-expressing cells. Depending on cofactors involved, phospho-SMAD1/5/8 can promote transcription, as with *ID1* and *ID3*, or repress transcription, as we propose for *MITF* (*9*). In melanomas *MITF* expression is tuned to a moderate level, allowing proliferation without triggering differentiation that would be accompanied by exit from the cell cycle (*8, 10*). Therefore, we speculate that *GDF6* and BMP signaling promote tumor formation by preventing terminal differentiation induced by high levels of *MITF*. Consistent with this possibility, we found that zebrafish embryos treated with DMH1 at a time when *gdf6a* and *gdf6b* are expressed in the neural crest (*11*) had increased expression of *mitfa* and *typr1b* and a significant expansion of melanocytes (Fig. 2J; Fig. S8A). Conversely, injection of *gdf6b* RNA into zebrafish embryos reduced *mitfa* expression (Fig. S8B-D).

Transcriptome data also indicated a role for *GDF6* in regulation of apoptosis. Specifically, gene set enrichment analysis (GSEA) revealed that *GDF6* expression negatively correlated with expression of apoptotic pathway genes in cells with *GDF6* modulation as well as in patient samples (Fig. 3A,B; Fig. S9A). In functional analyses, *GDF6* or *SMAD1* knockdown caused elevated melanoma cell death, whereas *GDF6* overexpression had a protective effect (Fig. 3C-E; Fig. S9B-F, S10). *GDF6*-overexpressing xenografts had a slightly increased Ki67

proliferative index, suggesting that the reduction in cell death did not result from the failure to generate new cells with the potential to die (Fig. S9G). Finally, the cell death caused by loss of *GDF6* was rescued upon *SMAD1DVD* expression (Fig. 3F; Fig. S11A-C). Together these data indicate that *GDF6*-dependent BMP signaling protects melanoma cells from death.

To identify factors that aid in *GDF6*-dependent melanoma cell survival, we focused on reciprocally regulated neural crest genes *SNAI2* and *SOX9*, which are known to regulate melanoma cell death (*12, 13*). Whereas *SNAI2* was not involved (Fig. S12), *SOX9* was an important target of *GDF6*-dependent pro-survival activity. Both in zebrafish embryos and human melanoma cells, *GDF6* and the BMP pathway negatively regulated *SOX9* expression (Fig. 3G; Fig. S13A-C). Epistasis analyses showed that *SOX9* knockdown rescued the cell growth defects and cell death caused by *GDF6* knockdown (Fig. 3H,I; Fig. S13D-G). These data indicate that *GDF6* represses *SOX9* expression, thereby inhibiting cell death and promoting tumor growth.

We next assessed *GDF6* protein expression in human melanomas and examined potential clinical implications. In our own patient cohort, high levels of GDF6 and nuclear phospho-SMAD1/5/8 proteins were present in human melanomas; however, normal melanocytes of adjacent skin (Fig. 4A,B) or tumor-infiltrating cells (Fig. S14) rarely expressed either. To determine whether GDF6 expression correlated with melanoma patient clinical characteristics, we used a tissue microarray with 104 patient melanoma tissue cores (78 primary melanomas and 26 metastatic melanomas). Consistent with the initial cohort, robust GDF6 expression was observed in 80% of these melanomas. Importantly, patients whose tumors at diagnosis expressed high amounts of GDF6 had a lower survival probability than did patients whose tumors expressed no or low GDF6 (Fig. 4C; Table S4). This association was driven primarily by patients in the primary melanoma cohort (Fig. S15), suggesting that GDF6 could be an early predictor of

patient outcome. *GDF6* promotes melanoma progression, and these immunohistochemistry data indicate that tumors expressing GDF6 are associated with a poorer prognosis.

In this study, we have discovered an indispensable role for *GDF6* and BMP signaling in promoting a trunk neural crest identity in melanomas. Reawakening this identity endows melanoma cells with a suite of pro-tumorigenic features. Mechanistically, *GDF6* acts via SMAD1/5/8-mediated BMP signaling to repress *MITF,* thereby blocking differentiation. As a part of this identity, *GDF6* represses expression of the pro-apoptotic factor *SOX9* (Model; Fig. 4D). Our zebrafish embryo data and additional developmental studies in other systems (reviewed in (*14*)) suggest that normal embryonic activities of *GDF6* are reawakened in melanomas to prevent differentiation and promote survival. Knockdown studies indicate that *GDF6* inhibition slows tumor growth. As a secreted molecule, GDF6 inhibition could be accomplished *in vivo* by a variety of means, including cell-impermeable therapies. While great strides have been made in melanoma treatment through the use of targeted therapies and immune checkpoint inhibitors, a majority of patients with advanced disease still succumb within five years of diagnosis. Targets such as GDF6 represent excellent therapeutic opportunities to further treat this lethal disease.

References and Notes:

1. C. K. Kaufman *et al.*, A zebrafish melanoma model reveals emergence of neural crest identity during melanoma initiation. *Science (New York, N.Y.)* **351**, aad2197 (2016).
2. E. E. Patton *et al.*, BRAF mutations are sufficient to promote nevi formation and cooperate with p53 in the genesis of melanoma. *Current biology : CB* **15**, 249-254 (2005).
3. R. Beroukhim *et al.*, The landscape of somatic copy-number alteration across human cancers. *Nature* **463**, 899-905 (2010).
4. W. M. Lin *et al.*, Modeling genomic diversity and tumor dependency in malignant melanoma. *Cancer research* **68**, 664-673 (2008).
5. S. Tsukamoto *et al.*, Smad9 is a new type of transcriptional regulator in bone morphogenetic protein signaling. *Scientific reports* **4**, 7596 (2014).
6. T. Sauka-Spengler, M. Bronner-Fraser, A gene regulatory network orchestrates neural crest formation. *Nature reviews. Molecular cell biology* **9**, 557-568 (2008).
7. M. J. Hendrix *et al.*, Reprogramming metastatic tumour cells with embryonic microenvironments. *Nature reviews. Cancer* **7**, 246-255 (2007).
8. K. S. Hoek, C. R. Goding, Cancer stem cells versus phenotype-switching in melanoma. *Pigment cell & melanoma research* **23**, 746-759 (2010).
9. J. Massague, J. Seoane, D. Wotton, Smad transcription factors. *Genes & development* **19**, 2783-2810 (2005).
10. N. Vandamme, G. Berx, Melanoma cells revive an embryonic transcriptional network to dictate phenotypic heterogeneity. *Frontiers in oncology* **4**, 352 (2014).

11. D. G. Howe *et al.*, ZFIN, the Zebrafish Model Organism Database: increased support for mutants and transgenics. *Nucleic acids research* **41**, D854-860 (2013).
12. O. Shakhova *et al.*, Antagonistic cross-regulation between Sox9 and Sox10 controls an anti-tumorigenic program in melanoma. *PLoS genetics* **11**, e1004877 (2015).
13. M. Kajita, K. N. McClinic, P. A. Wade, Aberrant expression of the transcription factors snail and slug alters the response to genotoxic stress. *Molecular and cellular biology* **24**, 7559-7566 (2004).
14. L. A. Williams, D. Bhargav, A. D. Diwan, Unveiling the bmp13 enigma: redundant morphogen or crucial regulator? *International journal of biological sciences* **4**, 318-329 (2008).
15. Q. Wu *et al.*, Transcriptional regulation during p21WAF1/CIP1-induced apoptosis in human ovarian cancer cells. *The Journal of biological chemistry* **277**, 36329-36337 (2002).
16. C. J. Ceol *et al.*, The histone methyltransferase SETDB1 is recurrently amplified in melanoma and accelerates its onset. *Nature* **471**, 513-517 (2011).
17. W. Deng *et al.*, SOX9 inhibits beta-TrCP-mediated protein degradation to promote nuclear GLI1 expression and cancer stem cell properties. *Journal of cell science* **128**, 1123-1138 (2015).
18. C. Gazin, N. Wajapeyee, S. Gobeil, C. M. Virbasius, M. R. Green, An elaborate pathway required for Ras-mediated epigenetic silencing. *Nature* **449**, 1073-1077 (2007).
19. M. C. Ramel, C. S. Hill, The ventral to dorsal BMP activity gradient in the early zebrafish embryo is determined by graded expression of BMP ligands. *Developmental biology* **378**, 170-182 (2013).

20. J. Wang, D. Duncan, Z. Shi, B. Zhang, WEB-based GEne SeT AnaLysis Toolkit (WebGestalt): update 2013. *Nucleic acids research* **41**, W77-83 (2013).

21. B. Zhang, S. Kirov, J. Snoddy, WebGestalt: an integrated system for exploring gene sets in various biological contexts. *Nucleic acids research* **33**, W741-748 (2005).

22. B. Langmead, C. Trapnell, M. Pop, S. L. Salzberg, Ultrafast and memory-efficient alignment of short DNA sequences to the human genome. *Genome biology* **10**, R25 (2009).

23. S. Heinz *et al.*, Simple combinations of lineage-determining transcription factors prime cis-regulatory elements required for macrophage and B cell identities. *Molecular cell* **38**, 576-589 (2010).

24. J. Feng, T. Liu, B. Qin, Y. Zhang, X. S. Liu, Identifying ChIP-seq enrichment using MACS. *Nature protocols* **7**, 1728-1740 (2012).

25. L. J. Zhu *et al.*, ChIPpeakAnno: a Bioconductor package to annotate ChIP-seq and ChIP-chip data. *BMC bioinformatics* **11**, 237 (2010).

26. M. Krzywinski *et al.*, Circos: an information aesthetic for comparative genomics. *Genome research* **19**, 1639-1645 (2009).

27. K. Howe *et al.*, The zebrafish reference genome sequence and its relationship to the human genome. *Nature* **496**, 498-503 (2013).

28. J. E. Collins, S. White, S. M. Searle, D. L. Stemple, Incorporating RNA-seq data into the zebrafish Ensembl genebuild. *Genome research* **22**, 2067-2078 (2012).

29. S. F. Altschul, W. Gish, W. Miller, E. W. Myers, D. J. Lipman, Basic local alignment search tool. *Journal of molecular biology* **215**, 403-410 (1990).

30. A. S, FastQC: a quality control tool for high throughput sequence data. (2010).

31. A. Dobin *et al.*, STAR: ultrafast universal RNA-seq aligner. *Bioinformatics (Oxford, England)* **29**, 15-21 (2013).

32. S. Anders, P. T. Pyl, W. Huber, HTSeq--a Python framework to work with high-throughput sequencing data. *Bioinformatics (Oxford, England)* **31**, 166-169 (2015).

33. M. E. Ritchie *et al.*, limma powers differential expression analyses for RNA-sequencing and microarray studies. *Nucleic acids research* **43**, e47 (2015).

34. B. Langmead, S. L. Salzberg, Fast gapped-read alignment with Bowtie 2. *Nature methods* **9**, 357-359 (2012).

35. D. Kim *et al.*, TopHat2: accurate alignment of transcriptomes in the presence of insertions, deletions and gene fusions. *Genome biology* **14**, R36 (2013).

36. H. Li *et al.*, The Sequence Alignment/Map format and SAMtools. *Bioinformatics (Oxford, England)* **25**, 2078-2079 (2009).

37. H. Thorvaldsdottir, J. T. Robinson, J. P. Mesirov, Integrative Genomics Viewer (IGV): high-performance genomics data visualization and exploration. *Briefings in bioinformatics* **14**, 178-192 (2013).

38. C. Trapnell *et al.*, Differential gene and transcript expression analysis of RNA-seq experiments with TopHat and Cufflinks. *Nature protocols* **7**, 562-578 (2012).

39. M. I. Love, W. Huber, S. Anders, Moderated estimation of fold change and dispersion for RNA-seq data with DESeq2. *Genome biology* **15**, 550 (2014).

40. C. Wilks *et al.*, The Cancer Genomics Hub (CGHub): overcoming cancer through the power of torrential data. *Database : the journal of biological databases and curation* **2014**, (2014).

41. Genomic Classification of Cutaneous Melanoma. *Cell* **161**, 1681-1696 (2015).

42. T. Barrett *et al.*, NCBI GEO: archive for functional genomics data sets--update. *Nucleic acids research* **41**, D991-995 (2013).

43. An integrated encyclopedia of DNA elements in the human genome. *Nature* **489**, 57-74 (2012).

Acknowledgments:

We thank Roger Davis, Eric Baehrecke, Nathan Lawson, Stephen Jones and Len Zon for helpful discussions. We thank Melissa Kasheta, Sarah Hainer, Thomas Fazzio, Fang Liu, Lin Lin, Paul Kaufman, Takenobu Katagiri, Patrick White , Ed Jaskolski, Karen Sargent, Jia Xu, Jiang-Liang Li, Feng Qi, and the UMMS DERC, Flow Cytometry and RNAi cores for experimental support. We acknowledge the ENCODE Consortium and Thomas Gingeras's lab for human melanocyte RNAseq data generation. C.B.F.G. was supported by Karina G. Zecchin and the CAPES program, Brazil. C.J.C. was supported by Kimmel Scholar Award SKF-13-123, DoD Career Development Award W81XWH-13-0107, Worcester Foundation Award P60016170000122, and the NIH NIAMS R01 AR063850-01. The content is solely the responsibility of the authors and does not necessarily represent the official views of the DoD or NIH. The data reported in this paper are tabulated in supplementary materials and/or deposited at Gene Expression Omnibus, ID GSE83400

Figure1

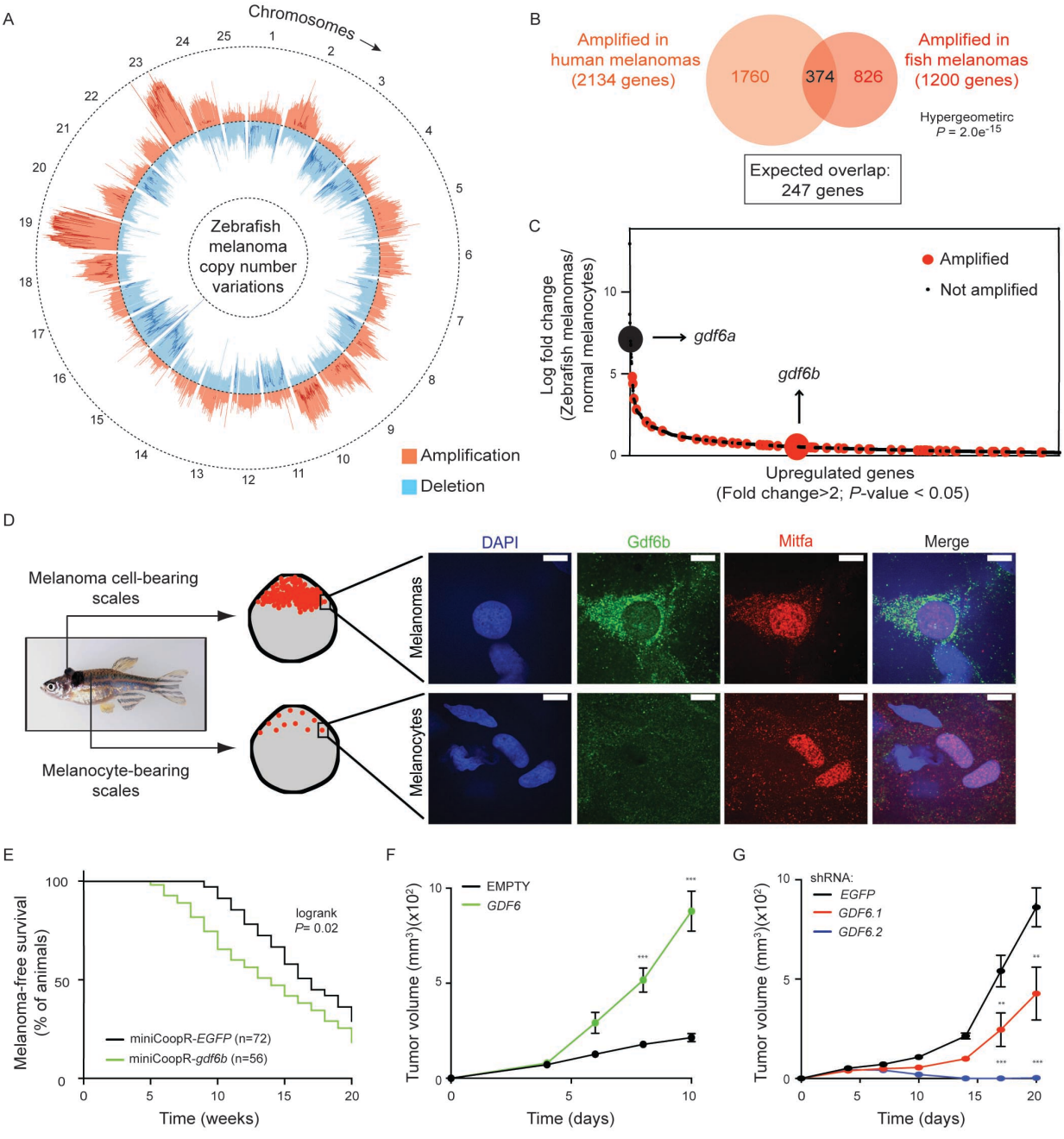
A
Chromosomes
Zebrafish melanoma copy number variations
Amplification
Deletion
B
Amplified in human melanomas (2134 genes)
1760
374
826
Amplified in fish melanomas (1200 genes)
Hypergeometirc P = 2.0e-15
Expected overlap: 247 genes
C
Log fold change (Zebrafish melanomas/ normal melanocytes)
Amplified
Not amplified
gdf6a
gdf6b
Upregulated genes
(Fold change>2; P-value < 0.05)
D
Melanoma cell-bearing scales
Melanocyte-bearing scales
DAPI
Gdf6b
Mitfa
Merge
Melanomas
Melanocytes
E
Melanoma-free survival (% of animals)
logrank P= 0.02
miniCoopR-EGFP (n=72)
miniCoopR-gdf6b (n=56)
Time (weeks)
F
Tumor volume (mm3)(x102)
EMPTY
GDF6
Time (days)
G
Tumor volume (mm3)(x102)
shRNA:
EGFP
GDF6.1
GDF6.2
Time (days)

Fig. 1. **Identification of *GDF6* as a melanoma oncogene**

(A) Circos plot displaying CNVs of zebrafish melanomas. –log10-transformed JISTIC Q-values (0.6 cut-off) are displayed as bold red (amplifications) and bold blue (deletions) lines. **(B)** Overlap of orthologous genes amplified in human and zebrafish melanomas from a total of 10380 human-zebrafish orthologous gene pairs. **(C)** Genes significantly upregulated in zebrafish melanomas as compared to melanocytes are plotted in order of their fold change. **(D)** Immunostaining of *Tg(mitfa:BRAF(V600E));p53(lf)* zebrafish scales bearing melanoma cells or normal melanocytes. Scale bar, 10 μm. **(E)** Melanoma-free survival curves for *Tg(mitfa:BRAF(V600E));p53(lf);mitfa(lf)* zebrafish injected with miniCoopR-*gdf6b* or miniCoopR-*EGFP*. **(F)** Mouse xenograft assay with *GDF6*-overexpressing A375 cells. **(G)** Mouse xenograft assay with *GDF6*-knockdown A375 cells. Error bars indicate s.e.m.; n=3. Two-tailed Student's t-test, $^{**}P < 0.01$, $^{***}P < 0.001$.

Figure2

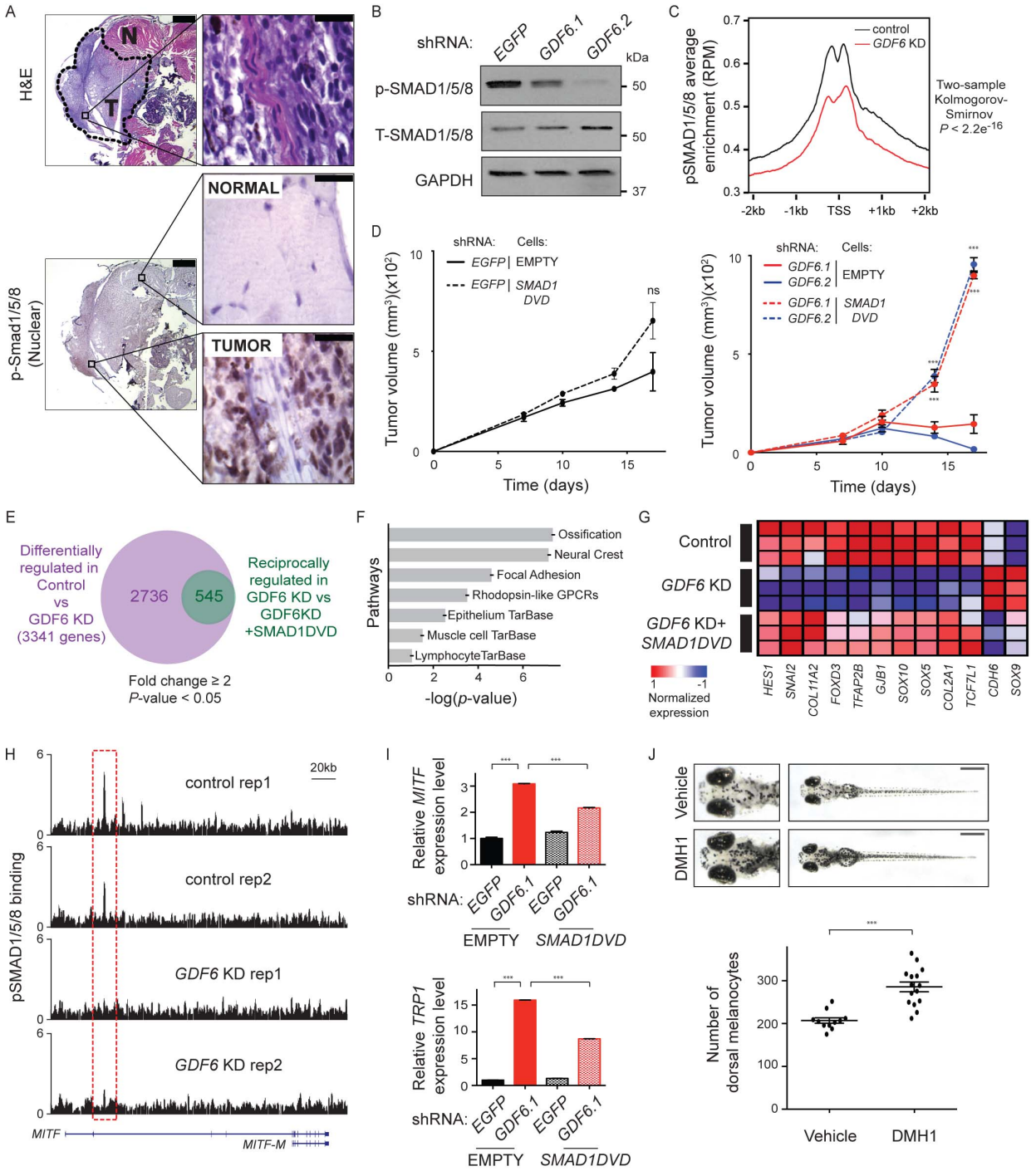
A
H&E
N
C
T
NORMAL
p-Smad1/5/8 (Nuclear)
TUMOR
B
shRNA:
EGFP
GDF6.1
GDF6.2
kDa
p-SMAD1/5/8
T-SMAD1/5/8
GAPDH
50
50
37
C
pSMAD1/5/8 average enrichment (RPM)
control
GDF6 KD
Two-sample Kolmogorov-Smirnov
P < 2.2e-16
-2kb
-1kb
TSS
+1kb
+2kb
D
shRNA:
Cells:
EGFP | EMPTY
EGFP | SMAD1 DVD
Tumor volume (mm3)(x102)
ns
Time (days)
GDF6.1 | EMPTY
GDF6.2 | EMPTY
GDF6.1 | SMAD1 DVD
GDF6.2 | SMAD1 DVD
E
Differentially regulated in Control vs GDF6 KD (3341 genes)
2736
545
Reciprocally regulated in GDF6 KD vs GDF6KD +SMAD1DVD
Fold change ≥ 2
P-value < 0.05
F
Pathways
Ossification
Neural Crest
Focal Adhesion
Rhodopsin-like GPCRs
Epithelium TarBase
Muscle cell TarBase
LymphocyteTarBase
-log(p-value)
G
Control
GDF6 KD
GDF6 KD+ SMAD1DVD
Normalized expression
HES1
SNAI2
COL11A2
FOXD3
TFAP2B
GJB1
SOX10
SOX5
COL2A1
TCF7L1
CDH6
SOX9
H
pSMAD1/5/8 binding
20kb
control rep1
control rep2
GDF6 KD rep1
GDF6 KD rep2
MITF
MITF-M
I
Relative MITF expression level
shRNA:
EGFP
GDF6.1
EGFP
GDF6.1
EMPTY
SMAD1DVD
Relative TRP1 expression level
J
Vehicle
DMH1
Number of dorsal melanocytes
Vehicle
DMH1

Fig. 2. *GDF6* acts via SMAD1 to induce a neural crest identity and inhibit differentiation in melanomas

(A) Stained transverse sections of a *Tg(mitfa:BRAF(V600E));p53(lf)* zebrafish bearing an invasive melanoma in the dorsal musculature. Left, scale bar, 500 μm. Right, scale bar, 50 μm. T, tumor. N, normal. **(B)** Immunoblots of *GDF6*-knockdown A375 cells. **(C)** Aggregation plot of phospho-SMAD1/5/8 ChIPseq binding at annotated TSSs in *GDF6*-knockdown A375 cells. **(D)** Tumor formation in mice injected with A375-empty or A375-*SMAD1DVD* cells expressing *shEGFP* (left) or with *GDF6* knockdown (right). **(E)** Genes differentially regulated upon *GDF6* knockdown (purple circle) and genes reciprocally regulated in *SMAD1DVD*-expressing cells upon *GDF6* knockdown (green circle). **(F)** Pathway analysis with the 545 reciprocally regulated genes. **(G)** Heat map of neural crest genes identified in pathway analysis. **(H)** phospho-SMAD1/5/8 ChIPseq reads across the *MITF* locus in *GDF6*-knockdown A375 cells. **(I)** qRT-PCR of *MITF* (top) and *TRP1* (bottom) in A375-empty or A375-*SMAD1DVD* cells with *GDF6* knockdown. Left brackets, expression is upregulated upon *GDF6* knockdown. Right brackets, expression is less upregulated in *SMAD1DVD*-expressing cells upon *GDF6* knockdown. **(J)** Top, epinephrine-treated zebrafish embryos at 5dpf incubated with DMSO vehicle control or 5μM DMH1. Scale bar: 500 μM. Bottom, melanocyte quantification. Error bars indicate s.e.m.; n=3. Two-tailed Student's t-test, ***P< 0.001. ns, not significant.

Figure3

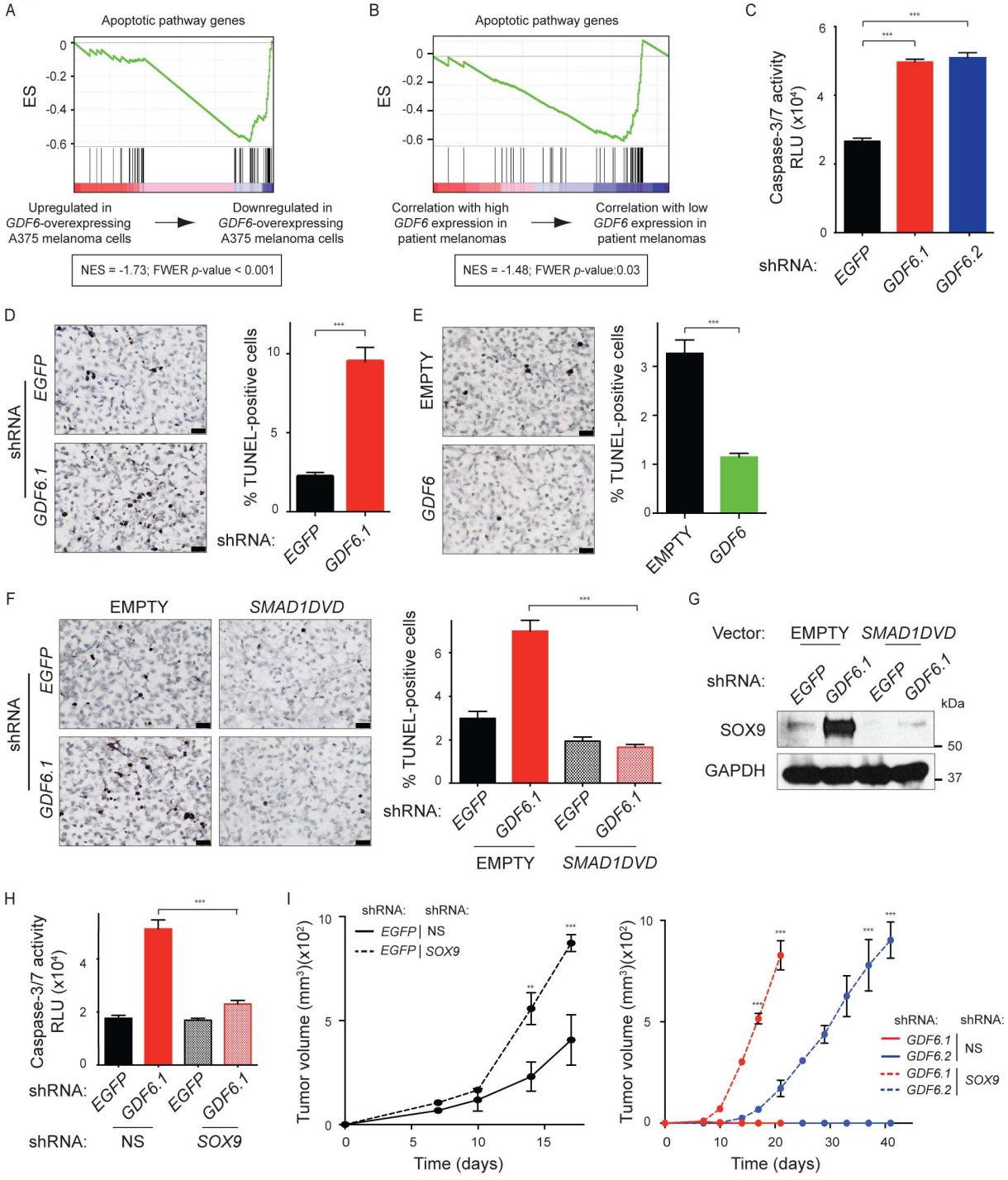
A
Apoptotic pathway genes
ES
Upregulated in GDF6-overexpressing A375 melanoma cells
Downregulated in GDF6-overexpressing A375 melanoma cells
NES = -1.73; FWER p-value < 0.001
B
Apoptotic pathway genes
ES
Correlation with high GDF6 expression in patient melanomas
Correlation with low GDF6 expression in patient melanomas
NES = -1.48; FWER p-value:0.03
C
Caspase-3/7 activity RLU (x10⁴)
shRNA: EGFP GDF6.1 GDF6.2
D
shRNA
EGFP
GDF6.1
% TUNEL-positive cells
shRNA: EGFP GDF6.1
E
EMPTY
GDF6
% TUNEL-positive cells
EMPTY GDF6
F
EMPTY
SMAD1DVD
shRNA
EGFP
GDF6.1
% TUNEL-positive cells
shRNA: EGFP GDF6.1 EGFP GDF6.1
EMPTY SMAD1DVD
G
Vector: EMPTY SMAD1DVD
shRNA: EGFP GDF6.1 EGFP GDF6.1
kDa
SOX9
GAPDH
50
37
H
Caspase-3/7 activity RLU (x10⁴)
shRNA: EGFP GDF6.1 EGFP GDF6.1
shRNA: NS SOX9
I
shRNA: shRNA:
EGFP | NS
EGFP | SOX9
Tumor volume (mm³)(x10²)
Time (days)
shRNA: shRNA:
GDF6.1 | NS
GDF6.2 | NS
GDF6.1 | SOX9
GDF6.2 | SOX9
Tumor volume (mm³)(x10²)
Time (days)

Fig. 3. *GDF6* and the BMP pathway repress *SOX9* expression to enable melanoma cell survival

(A) GSEA shows that expression of an apoptotic gene set (*15*) is negatively enriched in *GDF6*-overexpression A375 cells. **(B)** GSEA shows that expression of an apoptotic gene set (*15*) is negatively enriched in high *GDF6*-expressing patient-derived melanomas (TCGA). **(C)** Caspase-3/7 activity measured as relative luciferase units (RLU) in A375 cells upon *GDF6* knockdown. **(D)** TUNEL staining of mouse xenografts of A375 cells upon *GDF6* knockdown. Scale bar, 25µm. **(E)** TUNEL staining of mouse xenografts of A375 cells upon *GDF6* overexpression. Scale bar, 25µm. **(F)** TUNEL staining of mouse xenografts of A375 cells expressing *SMAD1DVD* upon *GDF6* knockdown. Scale bar, 25µm. **(G)** Immunoblots of A375-empty or A375-*SMAD1DVD* cells with *GDF6* knockdown. **(H)** Caspase-3/7 activity in A375-non-silencing or A375-*shSOX9* cells with *GDF6* knockdown. **(I)** Mouse xenograft assay with A375-non-silencing or A375-*shSOX9* cells expressing *shEGFP* (left) or *GDF6*-targeted shRNAs (right). Error bars indicate s.e.m.; *n*=3 in C, H, I; n= 100 fields in D, E, F. Two-tailed Student's *t*-test, $^{**}P< 0.01$, $^{***}P< 0.001$.

Figure4

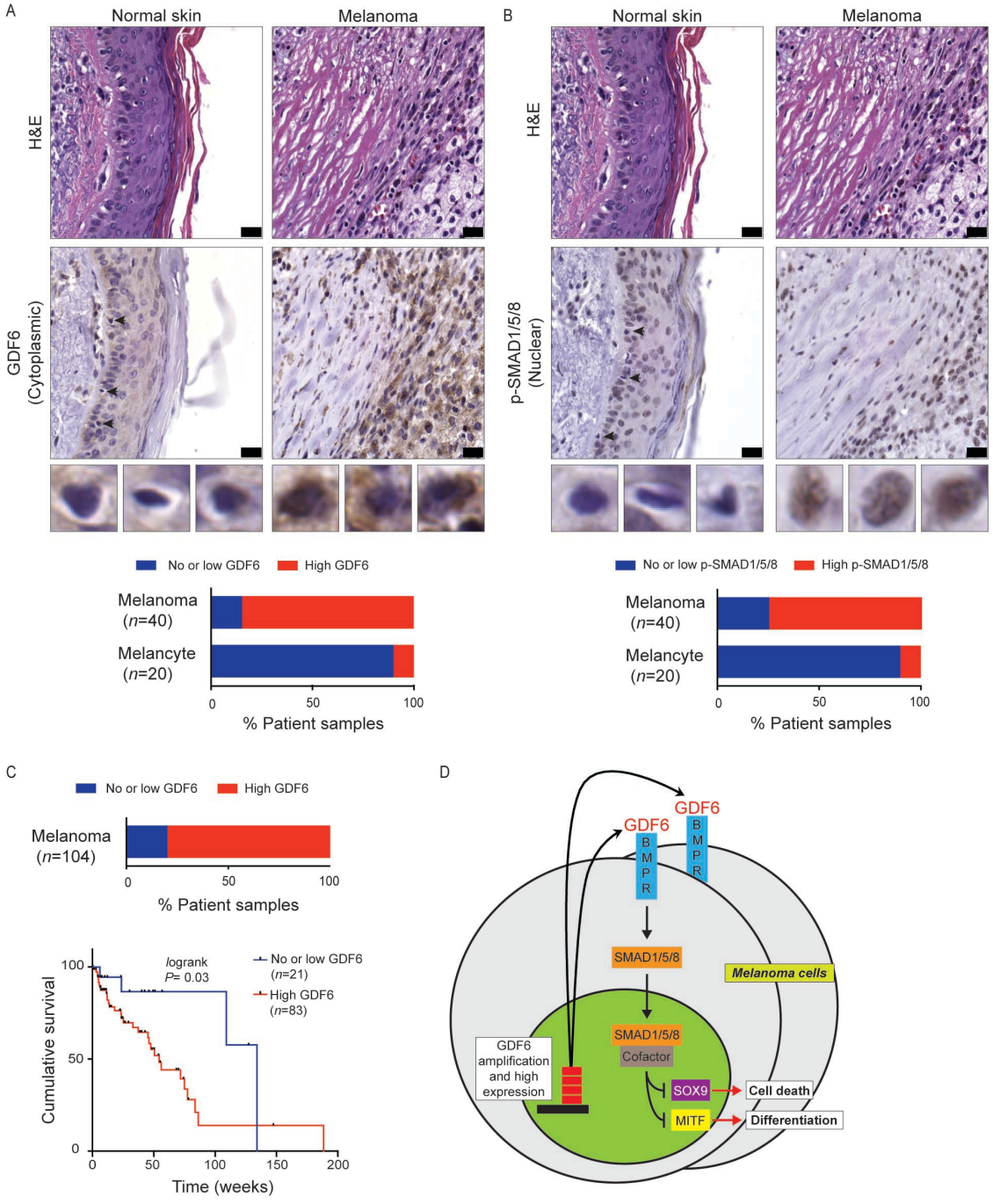
A
Normal skin
Melanoma
H&E
GDF6 (Cytoplasmic)
No or low GDF6
High GDF6
Melanoma (n=40)
Melancyte (n=20)
0
50
100
% Patient samples
B
Normal skin
Melanoma
H&E
p-SMAD1/5/8 (Nuclear)
No or low p-SMAD1/5/8
High p-SMAD1/5/8
Melanoma (n=40)
Melancyte (n=20)
0
50
100
% Patient samples
C
No or low GDF6
High GDF6
Melanoma (n=104)
0
50
100
% Patient samples
logrank P= 0.03
No or low GDF6 (n=21)
High GDF6 (n=83)
Cumulative survival
100
50
0
0
50
100
150
200
Time (weeks)
D
GDF6
GDF6
BMPR
BMPR
SMAD1/5/8
Melanoma cells
SMAD1/5/8
Cofactor
GDF6 amplification and high expression
SOX9
Cell death
MITF
Differentiation

Fig. 4. GDF6 expression is melanoma-specific and predicts patient outcome

(A) Stained human melanoma and adjacent skin samples. Melanocytes are indicated (arrowheads). Scale bar, 25µm. Individual cells are shown below. Bottom, quantification of samples based on GDF6 expression. **(B)** phospho-SMAD1/5/8 immunostaining of the same sample cohort. **(C)** Top, quantification of tissue microarray sample cohort based on GDF6 expression. Bottom, Kaplan-Meier analysis of patients with no or low versus high GDF6 expression. **(D)** Model for GDF6 activation and function in melanomas.

Supplementary Materials

www.sciencemag.org

Materials and Methods

Figs. S1 to S15

Tables S1 to S4

References 16-43

Supplementary Materials for:

Ligand-dependent BMP signaling reawakens an embryonic neural crest identity to promote melanoma

Arvind M. Venkatesan, Rajesh Vyas, Alec K. Gramann, Karen Dresser, Sharvari Gujja, Sanchita Bhatnagar, Sagar Chhangawala, Camilla Borges Ferreira Gomes, Hualin Simon Xi[1], Christine G. Lian, Yariv Houvras, Yvonne J. K. Edwards, April Deng, Michael Green & Craig J. Ceol*

*Corresponding author, email [Craig.Ceol@umassmed.edu]

This PDF file includes:

Materials and Methods
Figs. S1 to S15

Other Supplementary Materials for this manuscript includes the following:

Tables S1 to S4

Supplementary Materials

Materials and Methods:

Cell lines and cell culture

A375, MeWo and HEK293T cells (ATCC) were maintained in Dulbecco's Modified Eagle's Medium (DMEM) and SK-MEL-28 cells (ATCC) were maintained in Roswell Park Memorial Institute (RPMI) 1640 media supplemented with 10% fetal bovine serum (FBS) and 2 μg/ml Pen Strep (Gibco) at 37°C and 5% CO_2. Cells cultured at the same time were pooled, counted and then seeded in a 10cm dish. Wells/dishes were then subjected to treatment with lentiviral vectors.

Lentiviral infection

Lentiviral infections were performed as described previously (*16*). For stable gene knockdowns, we used pLKO-1 lentiviral vectors to deliver short hairpin sequences (shRNAs) (obtained from the RNAi Consortium (TRC)/Broad Institute through the UMMS RNAi core facility) specific for *GDF6* (GDF6.1: TRCN0000141818, target sequence: GCCAAGTGTTACATTGAGCTT; GDF6.2: TRCN0000140097, target sequence: GTGTCCATGCTCTCAGACAAA) or *SMAD1* (SMAD1.1: TRCN0000021781, target sequence: CGGTTGCTTATGAGGAACCAA; SMAD1.2: TRCN0000021782, target sequence: GCCGATGGACACAAACATGAT) or *EGFP* (TRCN0000072181, target sequence: ACAACAGCCACAACGTCTATA). Virus was made using a second generation lentiviral packaging system in HEK293T cells and quantified using a p24 ELISA kit (Clontech). Cells were infected with virus at a multiplicity of infection of 2.5 with 8 μg/ml polybrene followed by puromycin selection (2 μg/ml) for 2 days in appropriate media. For genetic epistasis experiments with *SOX9,* we used the pGIPZ lentiviral vectors (obtained

from Thermofisher Scientific through the UMMS RNAi core facility) to deliver shRNAs specific for *SOX9* (V3LHS_396212, target sequence: AGTCGTACTGTGAGCGGGT) or used the non-silencing control (target sequence: CTTACTCTCGCCCAAGCGAGAG) (*17*). A375 melanoma cells expressing an shRNA targeting *GDF6* or *EGFP* were treated with virus delivering *SOX9* or non-silencing shRNA. The viral dosage was determined such that 100% of the cells were EGFP-positive and therefore contained the pGIPZ vector expressing either *SOX9* or non-silencing shRNA. For transgene expression, we used Gateway cloning (Life Technologies) to insert the *GDF6* or *SNAI2* ORF (GE life sciences) or *SMAD1DVD* ORF (provided by Takenobu Katagiri) into the pLenti CMV Hygro DEST (w117-1) vector (provided by Paul Kaufman). Infection and monitoring was performed as described (*16*), except that selection was done with 300 ug/ml hygromycin for 10 days.

Mouse xenografts

All animal protocols were approved by the UMMS Institution Animal Care and Use Committee (A-2016, A-2171). Mice were randomly allocated to individual experimental groups. No blinding was done as animal groups were identified by tagging and cage labeling. Animals were excluded, according to pre-established criteria, if the tumor volume reached >1,000 mm^3; if tumor size or location affected the mobility or general health of animal, the animal was euthanized and excluded from the experiment or the complete experiment was terminated.

A375 cells stably expressing an *EGFP* or *GDF6* or *SMAD1* shRNA and/or empty vector or *GDF6*-expressing vector or *SMAD1DVD*-overexpressing vector were subcutaneously injected into the flanks of 6-8-week-old BALB/c nu/nu female mice (Taconic Farms) to produce orthotopic primary tumors. Primary tumor growth was monitored every 3 days with calipers, and

tumor volume was calculated as described previously (*18*). For *GDF6* knockdown, *SMAD1* knockdown and epistasis experiments with *SMAD1DVD* overexpression, 1 x 10^7 live cells were injected. For *GDF6* overexpression experiments and epistasis experiments with *SOX9* knockdown, 1 x 10^6 live cells were injected. For *GDF6* overexpression and *GDF6* knockdowns, a representative of two independent experiments (n=3 animals per experiment) is shown. For DMH1 drug experiments, 1 x 10^6 live A375 cells were subcutaneously injected in the flanks of BALB/c nu/nu female mice. Beginning on the day cells were injected, mice were injected intraperitoneally with vehicle (12.5% 2-hydroxypropyl-β-cyclodextrin) or 25 mg/kg DMH1 in vehicle every other day. This experiment was repeated twice and the weighted average of both experiments (n=8 animals total) is represented.

Growth curve, clonogenic and soft agar assays

For growth curves 50,000 live cells were seeded per well in a 6-well tissue culture plate on day 0. The numbers of live cells were calculated every day using an automated cell counter (Nexcelom Bioscience Cellometer Auto T4) following standard procedures. All assays were performed with technical replicates. For clonogenic assays, 3,000 live cells were seeded in a 10 cm tissue culture plate. After 3 weeks, colonies were fixed and stained using bromophenol blue in acetone. ImageJ was used to quantify the number of colonies. In assays with DMH1 treatment, control or DMH1-containing media was replaced every other day. For soft agar assays a 0.5% bottom layer (1:1 with 1% agar and 2XDMEM with 20% FBS) and a 0.3% top layer (1:1 with 0.6% agar and 2XDMEM with 20% FBS) were used. 3,000 live cells per well of a 6-well tissue culture plate were added in the top layer. Media was added initially then replaced every 3 days. After 3 weeks, colonies were stained with nitroblue tetrazolium chloride overnight at 37°C. Once

stained, individual wells were photographed, and ImageJ was used to count the number of colonies. All these assays were done in triplicate, and experiments were repeated at least twice.

Cell death assays

A375 melanoma cells after stable knockdown and/or overexpression were stained for Annexin V and 7-AAD (BD Pharmingen PR Annexin V Apoptosis Detection kit) as per manufacturer's instructions, followed by flow cytometry using a FACSCalibur instrument (BD Biosciences). Caspase3/7 activity was measured using the Caspase-Glo 3/7 assay (Promega) as per manufacturer's instructions.

miniCoopR assay

The miniCoopR assay measuring the effect of *gdf6b* on melanoma onset in zebrafish was performed as previously described (*16*). For miniCoopR-*EGFP* experiments a weighted average of two independent experiments is represented, and for miniCoopR-*gdf6b* experiments a weighted average of four independent experiments is represented.

Zebrafish drug experiments

Wild-type zebrafish embryos were collected and plated at a density of 50 embryos per 10cm tissue culture plate. At 10 hours post fertilization (hpf), embryos were dechorionated with pronase (400 ug/ml), rinsed 5 times with E3 water, and transferred to an agarose-bedded 6-well tissue culture plate at a density of 10 embryos per well. 5μM DMH1 or DMSO vehicle was immediately added to these wells. At 24hpf, drug was removed, embryos were rinsed 5 times

with E3 water and allowed to grow in the incubator. At 5 days post fertilization, embryos were treated with epinephrine (1mg/ml) in E3 water to contract melanosomes and were mounted on slides with 3% methylcellulose. Using a light microscope, the embryos were imaged and the number of dorsal melanocytes counted.

Zebrafish *gdf6b* RNA injections

Wild-type or *Tg(BRE:mRFP)* zebrafish embryos (*19*) were injected with 10 pg of *gdf6b* RNA (synthesized using the mMESSAGE mMACHINE SP6 Transcription Kit (Thermofisher)) in 1nl per embryo. For controls, embryos were mock injected with 1nl of distilled water. BMP pathway activity was monitored in *Tg(BRE:mRFP)* embryos with a fluorescent microscope at the 20 somite stage (20 *hpf*).

cDNA synthesis and qRT-PCR

For adult zebrafish, total RNA was extracted from melanoma cells and from normal scale-associated melanocytes of *Tg(mitfa:BRAF(V600E)); p53(lf); alb(lf); Tg(mitfa:EGFP)* zebrafish. For isolation of melanoma cells, melanomas were dissected, dissociated using Liberase TH treatment and subjected to fluorescence activated cell sorting (FACS) to isolate EGFP-positive cells. The same protocol was used for normal melanocytes, except dorsal scales from zebrafish were plucked to isolate melanocytes. Total RNA from zebrafish melanomas and melanocytes was isolated using Trizol-chloroform extraction, followed by RNA clean up (Qiagen RNeasy). Total RNA was reverse transcribed using the Superscript 2 Reverse Transcriptase kit (Invitrogen). qRT-PCR with SYBR green master mix (Biorad) was performed using the

following primers: *gdf6a* F: CTGAGAAACTGGGGCTCAAT, *gdf6a* R: CGACCAGCTCCTCTTTGTCT, *gdf6b* F: CGTCTAAAGCAGCAAACACC, *gdf6b* R: CCAAAGTGGAGAGTTCAAATGG, *actb1* F: CGAGCAGGAGATGGGAACC, *actb1* R: CAACGGAAACGCTCATTGC. For zebrafish embryos, drug treatment or RNA injections were performed as previously mentioned, except, for drug experiments 10μM DMH1 was used and total RNA was isolated at 20 hpf in the same manner. qRT-PCR was performed using the following primers: *mitfa* F*:* CTGGACCATGTGGCAAGTTT*, mitfa* R: GAGGTTGTGGTTGTCCTTCT, *tyrp1b* F: CGACAACCTGGGATACACCT, *tyrp1b* R: AACCAGCACCACTGCAACTA, *sox9b* F: TGACGAGTTGTTCTCCAGAG, *sox9b* R: AGGCCACACGTCTATAACCC.

For A375 human melanoma cells with *GDF6* and/or *SMAD1DVD* modulation, total RNA was prepared in the same manner, and qRT-PCR was performed using the following primers: *ID1* F: CCAACGCGCCTCGCCGGATC, *ID1* R: CTCCTCGCCAGTGCCTCAG, *ID3* F: CTGGACGACATGAACCACTG, *ID3* R: GTAGTCGATGACGCGCTGTA, *SNAI2* F: TGTTGCAGTGAGGGCAAGAA, *SNAI2* R: GACCCTGGTTGCTTCAAGGA, *SOX9* F: GTACCCGCACTTGCACAAC, *SOX9* R: TCTCGCTCTCGTTCAGAAGTC, *MITF* F: AAACCCCACCAAGTACCACA, *MITF* R: ACATGGCAAGCTCAGGAC, *TRP1* F: GTAACAGCACCGAGGATGG, *TRP1* R: TCCAAGCACTGAGCGACAT, *GAPDH* F: TGCACCACCAACTGCTTAGC, *GAPDH* R: GGCATGGACTGTGGTCATGAG.

Antibody production

Antibodies recognizing Gdf6b were generated by injecting a glutathione S-transferase-tagged *gdf6b*, GST-*gdf6b*, into two guinea pigs. Antibodies were validated by comparing reactivity of

pre- and post-immune sera to bacterially-expressed GST-*gdf6b*. Results from one of the antibodies are shown.

Immunofluorescence

For adults, dorsal scales bearing normal melanocytes or melanomas were plucked from anesthetized zebrafish. After fixation, scales were bleached of melanin pigment to visualize fluorescence after staining. Scales were incubated with primary antibody (Gdf6b (1:250), Mitfa (1:250)) overnight. Subsequently the scales were washed, incubated in appropriate secondary antibodies (Jackson Labs), incubated with DAPI, mounted on slides with Vectashield (Vectorlabs), and visualized using confocal fluorescence microscopy.

Immunoblotting

Protein extracts were separated on 12% SDS-PAGE gels. Blots were probed with primary antibodies (GDF6 (Sigma PRS4691; 1:1000), phospho-SMAD1/5/8 (Cell Signaling 13820; 1:1000), SMAD1 (Cell Signaling 9743; 1:500), Total SMAD1/5/8 (Santa Cruz sc-6031-R; 1:1000), FLAG (Sigma F3165, 1:2000), SOX9 (Cell Signaling 82630S; 1:1000), GAPDH (Abcam 8245; 1:2000)) overnight at 4°C, washed five times in TBS plus 0.1% Tween (TBST) and then incubated with the appropriate HRP-conjugated secondary antibody (Jackson Labs) for 1 hour at room temperature. Membranes were washed five times in TBST and visualized on autoradiography film after incubating with ECL reagent (Supersignal West Pico or Supersignal West Femto; Thermo Scientific).

Immunohistochemistry (IHC) and TUNEL staining

From mouse xenografts, formalin-fixed, paraffin-embedded tissues were processed to obtain 5μm sections. Sections were stained with H&E, cleaved Caspase-3 (Cell signaling 9664; 1:100), Ki-67 (Dako M7240; 1:100) and evaluated. TUNEL staining was performed on sections using the In Situ Cell Death Detection kit (Roche) as per manufacturer's protocol. The numbers of TUNEL-positive or cleaved Caspase-3-positive or Ki67-positive cells were counted manually and the total number of cells in each field was calculated using ImageJ software.

Individual patient melanoma and tissue microarray cores consisted of 5 μm sections of formalin-fixed, paraffin-embedded tissues. Slides were first deparaffinized with two changes of xylene, and rehydrated with changes of decreasing concentrations of alcohols, then rinsed in distilled water. Antigen retrieval was carried out with 0.01M citrate buffer at pH 6.0, or 0.001M EDTA at pH 8.0. Slides were heated in a 770W microwave oven for 14 minutes, cooled to room temperature, and rinsed in distilled water. The sections were first blocked for endogenous non-specific protein and peroxidase activity with an application of Dual Endogenous Block (Dako) for 10 minutes, followed by a buffer wash, followed by staining with antibodies recognizing GDF6 (Sigma PRS4691; 1:1000) and phospho-SMAD1/5/8 (Cell signaling 9664; 1:100) for 30 minutes. Staining with a second antibody recognizing GDF6 (Sigma HPA045206; 1:100) yielded concordant results. For negative controls, non-immune immunoglobulin G (a cocktail of Mouse Whole IgG and Rabbit Whole IgG (Pierce antibodies 31204 and 31207, respectively; both 1ug/ml)) staining was used. Following a buffer wash, sections were incubated with the EnVision+ Dual Link (Dako) detection reagent for 30 minutes. The sections were washed, and treated with a solution of diaminobenzidine and hydrogen peroxide (Dako) for 10 minutes, to produce the visible brown pigment. After rinsing, a toning solution (DAB Enhancer, Dako) was

used for 2 minutes to enrich the final color. The sections were counterstained with hematoxylin, dehydrated, and coverslipped with permanent mounting media. Positive signal was defined as dark brown staining. Scant, or fine granular background staining, or no staining was considered negative.

Zebrafish formalin-fixed, 5mM EDTA treated, paraffin-embedded tissues were processed to obtain 5μm transverse sections. Sections were stained as mentioned above with phospho-SMAD1/5/8 (Cell Signaling 9511; 1:150) and also counterstained with hematoxylin, dehydrated, and coverslipped with permanent mounting media.

IHC scoring

For both the UMass patient cohort and the tissue microarray, a modified visual semi-quantitative method was used. Sections were scored for immunointensity (0-4) and immunopositivity (0-3), which were then multiplied. For the UMMS patient cohort, scoring was done by C.J.C. and A.M.V., and the scores were averaged. Scores were verified by A.D. For the tissue microarray cohort, scoring was conducted independently by C.L. and C.B.F.G. and the scores were averaged. Sections with scores less than or equal to four were binned into the low or no staining group and sections with scores greater than four were binned into the high staining group.

Gene set enrichment analysis (GSEA) and pathway analysis

For GSEA, the enrichment score (ES), normalized enrichment score (NES) and familywise error rate (FWER) were calculated based on a running metric, which increased when a gene (vertical line in the graphical representation) in the gene set was encountered and decreased when one was

not. For GSEA of the apoptotic pathway gene signature (*15*), a rank-ordered gene list was made with FPKM values from *GDF6*-overexpressing A375 melanoma cells as compared to empty vector control cells or A375 cells expressing an shRNA targeting *EGFP* as compared to *GDF6.1* shRNA-expressing cells. Default parameters of GSEA were used and the Student's *t*-test was used to calculate significance. For GSEA based on TCGA samples, a rank-ordered gene list was derived from the expression profiles of 385 melanoma samples, using *GDF6* expression level as a continuous variable. Default parameters of GSEA were used, and Pearson correlation was used to calculate significance. Pathway analysis was performed using the WEB-based Gene SeT AnaLysis Toolkit (WebGestalt) (*20, 21*). Default parameters were used, except the minimum number of genes for a category was set to 10 and an adjusted *P*-value cut-off of 0.01 was used.

Chromatin immunoprecipitation (ChIP) sequencing and analysis

ChIP was performed using the Simple ChIP Plus Enzymatic Chromatin IP kit as per manufacturer's instructions (Cell Signaling 9001) with the phospho-SMAD1/5/8 antibody (Cell Signaling 11971; 1:100). ChIP-DNA from A375 melanoma cells expressing an shRNA targeting *GDF6, GDF6.1* or *EGFP* or a 2% input control was used for library preparation using the TruSeq ChIP Library Prep Kit for ChIP-Seq (Illumina). Fastq files were aligned to the human reference genome (ENSEMBL GRCH37) by Bowtie (version 1.0.0) (*22*) allowing uniquely mapped reads and removing PCR duplicates. For aggregation plotting, aligned reads were processed in HOMER (*23*) using annotatePeaks to bin the regions of interest in 20-bp windows resulting in average enrichment with normalized reads for all genes. MACS2 (version 2.1.1.20160226) (*24*) was used for peak calling. Peaks with a false discovery cutoff of 1% were used. The alignment files were converted to bedGraph files and loaded as custom tracks in the

UCSC genome browser to visualize regions of interest. ChIPpeakAnno (version 3.5.12) (*25*) was used to visualize and compare the overlapping pSMAD1/5/8 peaks for genes bound by pSMAD1/5/8 in wild-type and *GDF6* knockdown A375 cells. The *P-value* was calculated using the Kolmogorov-Smirnov tests after summing TSS-proximal reads for each gene (n=49,344 TSSs).

aCGH probe design

We custom designed the G3 array format of 2x400K probes for the Zebrafish ZV9 genome assembly using Agilent's eArray (eArray ID 036041). The array has 398426 unique probes covering 97% of the zebrafish genome (based on Zv9 assembly). The probes are 60 bases long and are spaced across the genome with an average separation of 3550 bases.

aCGH, JISTIC analysis and comparative analysis

aCGH was performed as per Agilent's array-based genomic DNA hybridization protocol. Briefly, genomic DNA was extracted from zebrafish melanomas or a normal region of the same fish using the Qiagen DNeasy Blood and Tissue kit. 5 µg of tumor or matched normal gDNA was fragmented to 200-500bp by sonication (Covaris S220R High Performance Sample Preparation Ultrasonicator System 220x S), labeled in a random-primed reaction using Cy5-dCTP or Cy3-dCTP, respectively, and hybridized in Agilent's hybridization buffer with Cot1 DNA (1mg/ml) at 65°C overnight. Arrays were then washed, and Cy5 and Cy3 signals were measured using an Agilent G2565 Microarray Scanner. Raw data was generated from scanned images with the Agilent Feature Extraction software (v10.7). Raw values were normalized using

the Agilent Genomic workbench and copy number alterations were detected. The JISTIC algorithm was used in limited peel-off mode to calculate significantly altered regions, and peak calling was done using a q-value cut-off of 0.25. Gene-based JISTIC G-scores and –log10 transformed q-values are represented using the Circos package (*26*). For representation of data, the G-score scale for amplifications was 0 (minimum) and 1550 (maximum), and for deletions it was 0 (minimum) and 2150 (maximum). The -log10-transformed q-value scale for both amplifications and deletions was 0 (minimum) and 11 (maximum). In Fig. 1A, dotted circles represent -log10-transformed q-value of 0 (center) and 11 (outer: amplification and inner: deletion). For human melanomas, copy number data was downloaded from Tumorscape (*3, 4*), and JISTIC analysis was conducted as described above. Genes from within peaks were pooled to define species-specific sets of recurrently amplified genes. Human orthologs of zebrafish genes were determined using Ensembl (*27, 28*) and supplemented by performing BLAST (*29*). Recurrently amplified zebrafish and human genes, as determined by JISTIC, were compared to find the overlapping set of commonly amplified genes.

cDNA amplification and microarray analysis

Total RNA was extracted and prepared from melanoma cells and from normal scale-associated melanocytes of *Tg(mitfa:BRAF(V600E)); p53(lf); alb(lf); Tg(mitfa:EGFP)* zebrafish as described above. Total RNA was amplified using the Nugen Ovation RNA Amplification system V2 as per manufacturer's protocol. For microarrays, amplified cDNA was hybridized to a 385K microarray (NimbleGen 0711105Zv7EXPR) as per manufacturer's protocol. Briefly, amplified cDNA from melanomas and melanocytes were labeled with Cy3 independently, hybridized to the microarray,

washed and scanned with a GenePix 4000B Scanner. Images were analyzed and normalized using NimbleScan software, and differentially expressed genes were identified.

Massively parallel RNA sequencing

For zebrafish melanomas and melanocytes, total RNA was isolated as described above and libraries were prepared using the TrueSeq Stranded mRNA Library Prep Kit as per manufacturer's protocol (Illumina). FASTQ files were analyzed using FASTQC v0.10.1(*30*) to ensure uniform read quality (phred>30). Paired-end reads were aligned to the zebrafish genome using STAR v2.3 (*31*) (Zv9). The mapped reads were counted using htseq-count (v0.6.0, parameters –t exon) (*32*) and gene models from the Ensembl transcriptome (*27*). Analyses of differential gene expression were performed using DESeq2 (*33*). Orthology to human genes was determined using Ensembl (*27, 28*) and supplemented by performing BLAST (*29*). The heatmap of BMP pathway genes (REACTOME_SIGNALING_BY_BMP; MSigDB (Broad Institute)) was created using human orthologs of differentially expressed BMP pathway genes. The fish orthologs of human genes represented are *SMAD5=smad5, SMAD4=si:dkey-239n17.4, ACVR2A=acvr2a, ACVR2B=acvr2b, BMPR1A=bmpr1aa, FSTL1=fstl1b, SMAD7=smad7, BMPR2=bmpr2a, SMURF2=smurf2, SMAD6=smad6b, ZFYVE16=zfyve16, SKI=skib, GREM2=grem2, SMURF1=smurf1, UBE2D1=ube2d1, CER1=dand5, NOG=nog, BMP2=bmp2b, BMPR1B=bmpr1bb*. For A375 human melanoma cells with *GDF6* and/or *SMAD1DVD* modulation, total RNA was isolated and libraries prepared as described above. Prepared libraries were sequenced using Illumina Hiseq technology (NY Genome Center). FASTQC v0.10.1 (*30*) was used on the FASTQ sequences for the A375 samples to generate sequence quality reports. Data were analyzed using two different bioinformatics pipelines. In the first pipeline, reads were aligned to the human reference genome (Ensembl GRCh37) using Bowtie2 (v 2-2.1.0) (*34*) and

Tophat2 (v 2.0.9) (*35*). Samtools (v 0.0.19) (*36*) and IGV (v 2.3.60) (*37*) were used for indexing the alignment files and viewing the aligned reads, respectively. Gene expression was quantitated as fragments per kilobase of exon model per million mapped fragments (FPKM) using Cufflinks (v 2.2.0) (*38*). Differentially-expressed genes were identified using the Cufflinks tools (Cuffmerge and Cuffdiff). cummeRbund (v 2.4.1) (*38*) was used to assess replicate concordance. In the second pipeline, reads were mapped against the human reference genome (Ensembl GRCh37) using the aligner STAR (v 2.4.2a), and gene level counts of uniquely mapped reads were obtained using htseq-count (v 0.6.1) (*32*). Differential expression analysis was performed using DESeq2 (*39*) for each pairwise condition using a p-adj threshold of 0.05. The FPKM-based method and the counts-based method generated concordant results. Analyses using the FPKM-based method have been represented in results.

Human melanocyte and melanoma transcriptome analysis

Three hundred and eighty-five human RNA-seq samples were downloaded from the Cancer Genomics Hub (CGHub) (https://cghub.ucsc.edu) using GeneTorrent (v 3.8.5a) (*40*). The RNAseq TCGA dataset is comprised of three sample types: 302 metastatic melanoma samples, 82 primary melanomas, and 1 solid tissue normal (*41*). For the normal melanocyte datasets, two RNAseq samples were downloaded from the Short Read Archive (SRA) (https://www.ncbi.nlm.nih.gov/sra/; accession codes: SRR522118, SRR522119)(*42*) and two from the ENCODE project (https://www.encodeproject.org/; experiment: ENCSR000CUQ) (*43*). The datasets downloaded from TCGA, SRA and ENCODE were aligned to the human reference genome (Ensembl GRCh37) and analyzed using the FPKM-based method described above.

SUPPLEMENTAL FIGURE 1

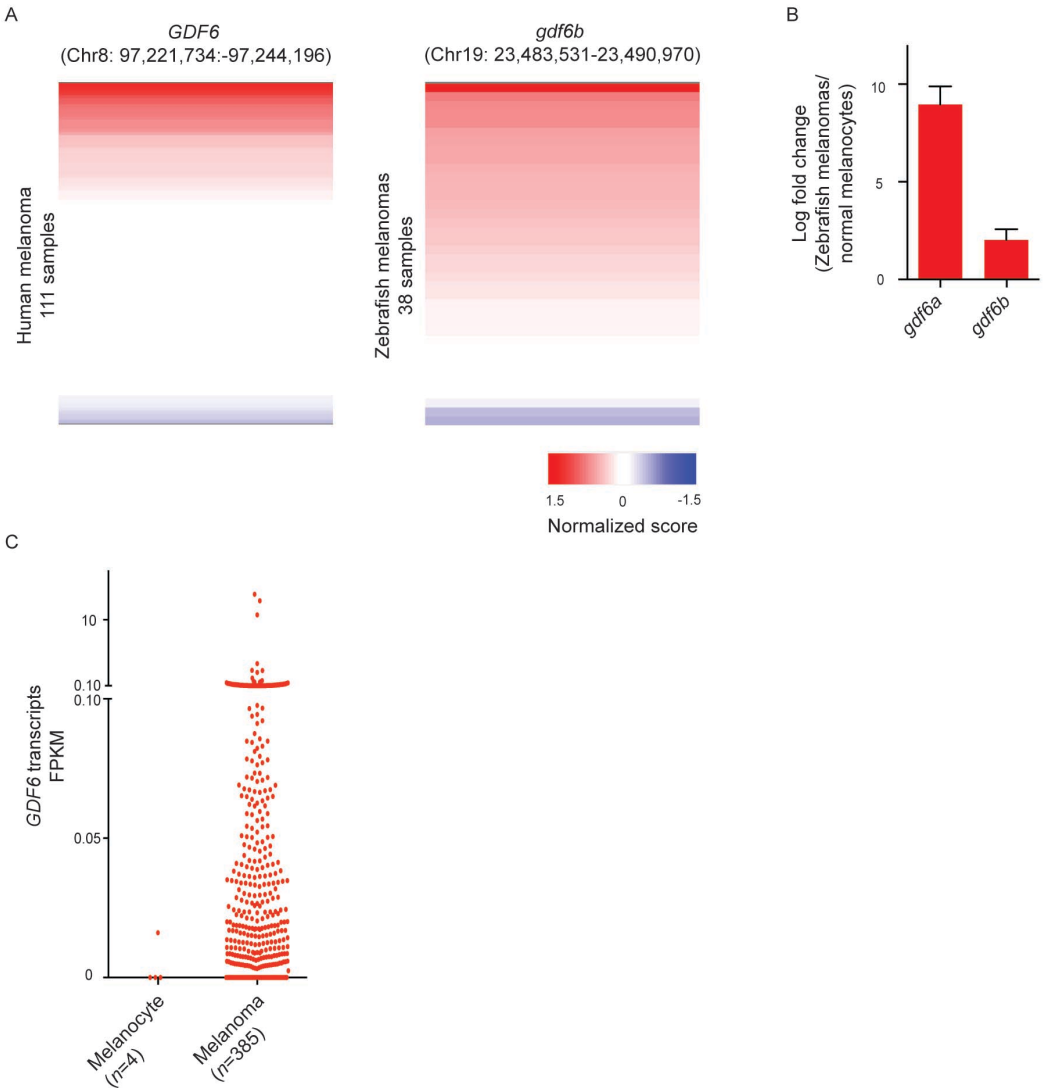

Fig. S1. *GDF6* orthologs are amplified and upregulated in human and zebrafish melanomas

(A) Left, heat map showing copy number of the human *GDF6* locus across 111 human melanomas. Right, heatmap showing copy number of the zebrafish *gdf6b* locus across 38 zebrafish melanomas. Red indicates amplification, blue indicates deletion. (B) Log2-transformed fold change of *gdf6a* and *gdf6b* expression in zebrafish melanomas as compared to melanocytes as determined by qRT-PCR. (C) *GDF6* transcript FPKM values of normal human melanocytes and melanomas.

SUPPLEMENTAL FIGURE 2

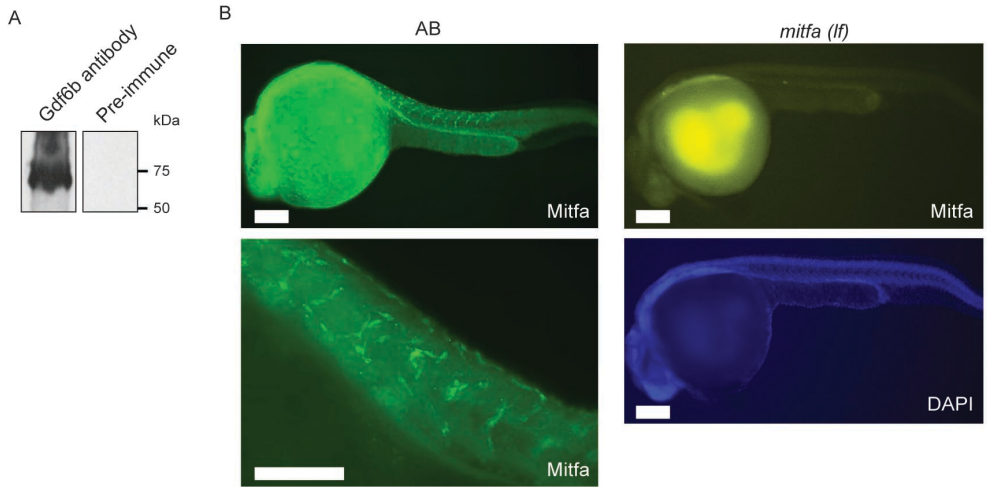

Fig. S2. Specificity of zebrafish Gdf6b and Mitfa antibodies

(A) Immunoblots with recombinant GST-Gdf6b-expressing bacterial cell lysate using Gdf6b antibody (left) and pre-immune serum (right). The GST-Gdf6b molecular weight is predicted to be 73 kD. (B) Left, Immunostaining with Mitfa antibody in wild-type AB zebrafish embryos. Right, Immunostaining with Mitfa antibody in *mitfa(lf)* zebrafish embryos. Mitfa (top), DAPI (bottom). Scale bars, 100 uM.

SUPPLEMENTAL FIGURE 3

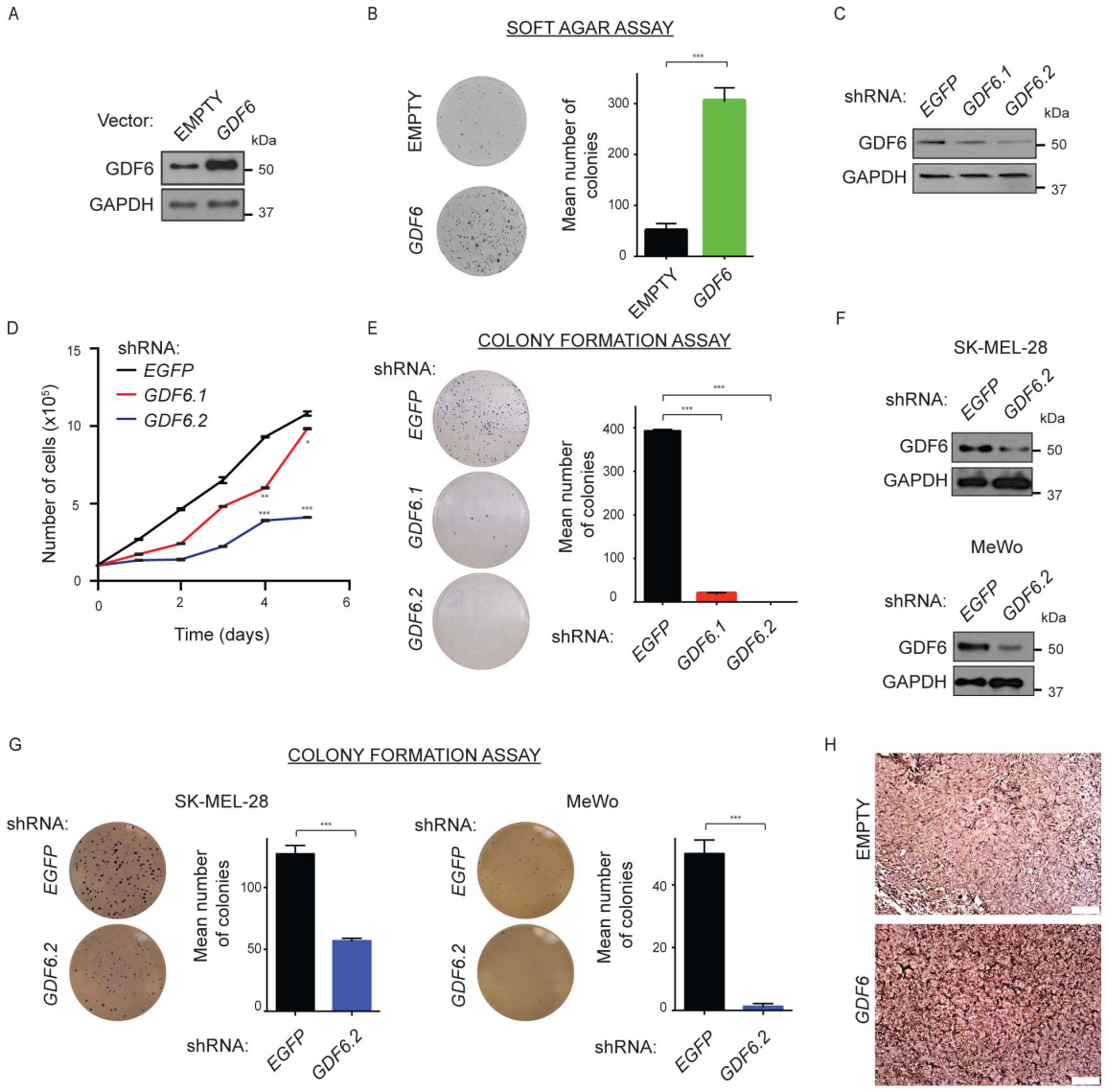

Fig. S3. *GDF6* modulation affects melanoma cell growth

(A) Immunoblots showing expression of GDF6 and GAPDH in A375 melanoma cells overexpressing *GDF6* or empty vector control. **(B)** Soft agar assay with A375 cells overexpressing *GDF6* or empty vector control. Growth in culture and colony formation were not affected by *GDF6* overexpression (data not shown). **(C)** Immunoblots showing expression of GDF6 and GAPDH in A375 melanoma cells expressing an shRNA targeting *EGFP* or two independent *GDF6*-targeted shRNAs. **(D)** Growth curves of A375 cells expressing *shEGFP*, *shGDF6.1* or *shGDF6.2*. **(E)** Colony formation assay with A375 cells expressing an shRNA targeting *EGFP* or two independent *GDF6*-targeted shRNAs. **(F)** Immunoblots of GDF6 and GAPDH in SK-MEL-28 melanoma cells (top) and MeWo melanoma cells (bottom) expressing *shEGFP* or *shGDF6.2*. **(G)** Colony formation assay with SK-MEL-28 melanoma cells (left) and MeWo melanoma cells (right) expressing *shEGFP* or *shGDF6.2*. **(H)** GDF6 staining of mouse xenografts of A375 cells showing elevated levels of GDF6 in *GDF6*-overexpressing xenografts compared to controls. Scale bars, 50 μm. Error bars indicate s.e.m.; n=3. Two-tailed Student's t-test, $^{*}P< 0.05$, $^{**}P< 0.01$, $^{***}P< 0.001$.

SUPPLEMENTAL FIGURE 4

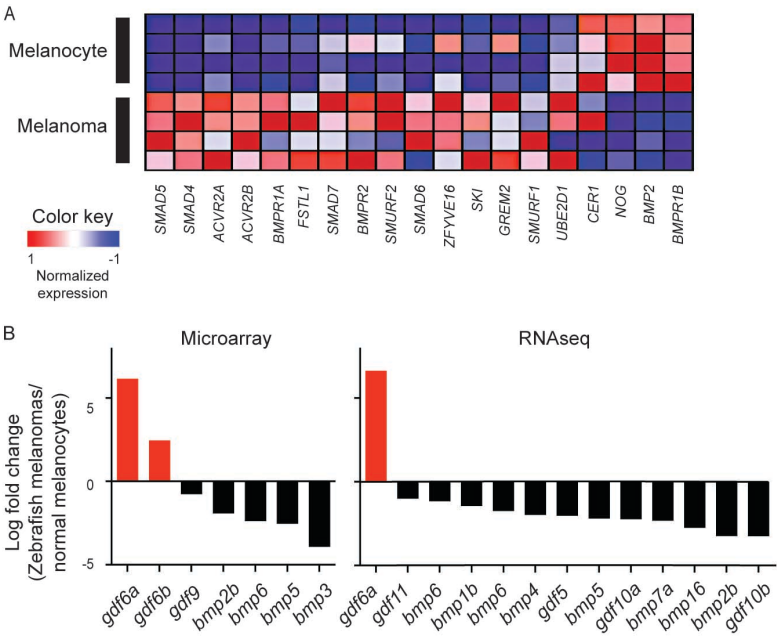

Fig. S4. Expression of BMP pathway components in zebrafish melanomas and melanocytes

(A) Heat map of gene expression of BMP pathway genes (Reactome gene set) in zebrafish melanomas compared to melanocytes. **(B)** log2-transformed fold change of gene expression in zebrafish melanomas as compared to melanocytes (y-axis). BMP ligands (p-value<0.05) in microarray analysis (left) and RNAseq analysis (right).

SUPPLEMENTAL FIGURE 5

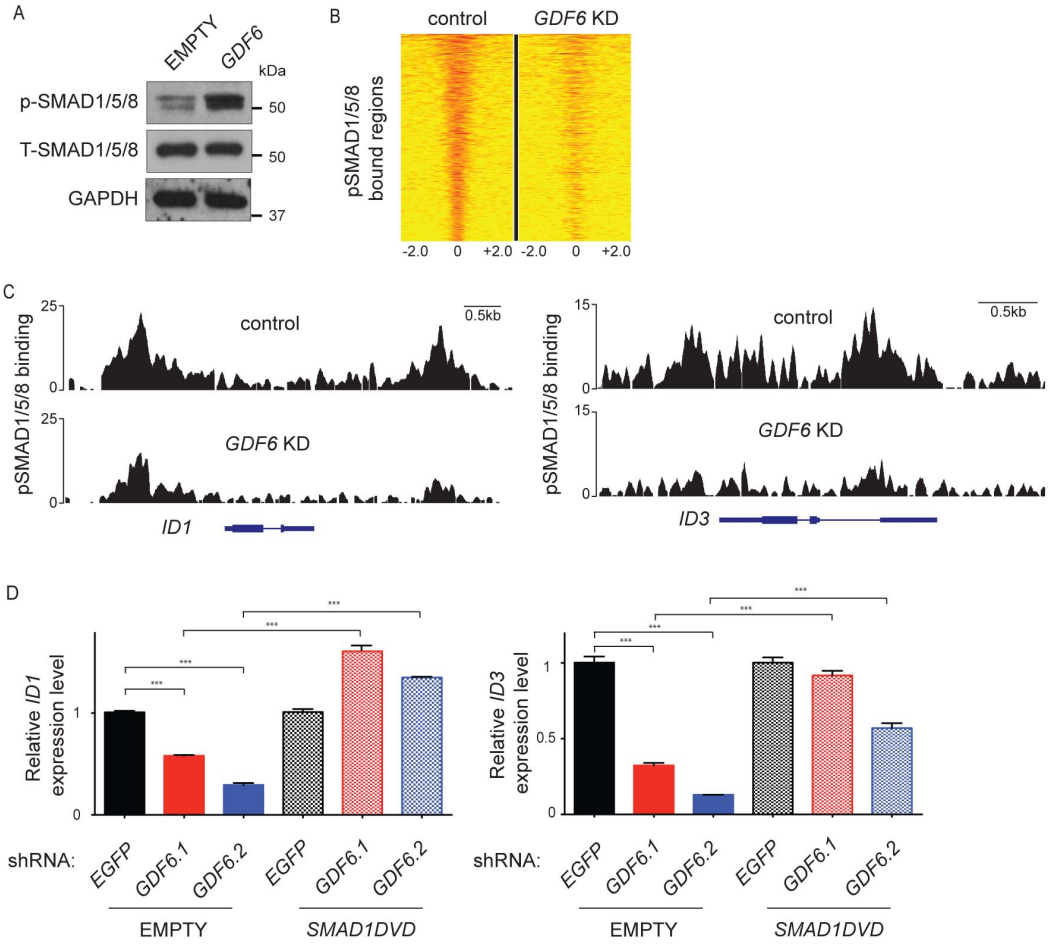

Fig. S5. *GDF6* knockdown abrogates phospho-SMAD1/5/8 DNA binding in A375 melanoma cells

(A) Immunoblots of *GDF6*-overexpressing A375 cells. **(B)** Comparison of ChIPseq maps of phospho-SMAD1/5/8 binding in control and *GDF6*-depeleted cells. The heat map extends from -2kb to +2kb from the context of each bound region, with each row representing a unique bound region and enrichment denoted in red. The heat map is sorted based on phsopho-SMAD1/5/8 binding in control cells. **(C)** phospho-SMAD1/5/8 binding to the *ID1* locus (left) and *ID3* locus (right) in A375 melanoma cells expressing *shEGFP* or *shGDF6.1*. **(D)** qRT-PCR showing expression of *ID1* (left) and *ID3* (right) in A375-empty or A375-*SMAD1DVD* cells expressing an shRNA targeting *EGFP* or two independent *GDF6*-targeted shRNAs. Left two brackets, *ID* gene expression is downregulated upon *GDF6* knockdown. Right two brackets, downregulation of *ID* gene expression is reversed in *SMAD1DVD*-expressing cells upon *GDF6* knockdown. Error bars indicate s.e.m.; n=3. Two-tailed Student's t-test, ***P< 0.001.

SUPPLEMENTAL FIGURE 6

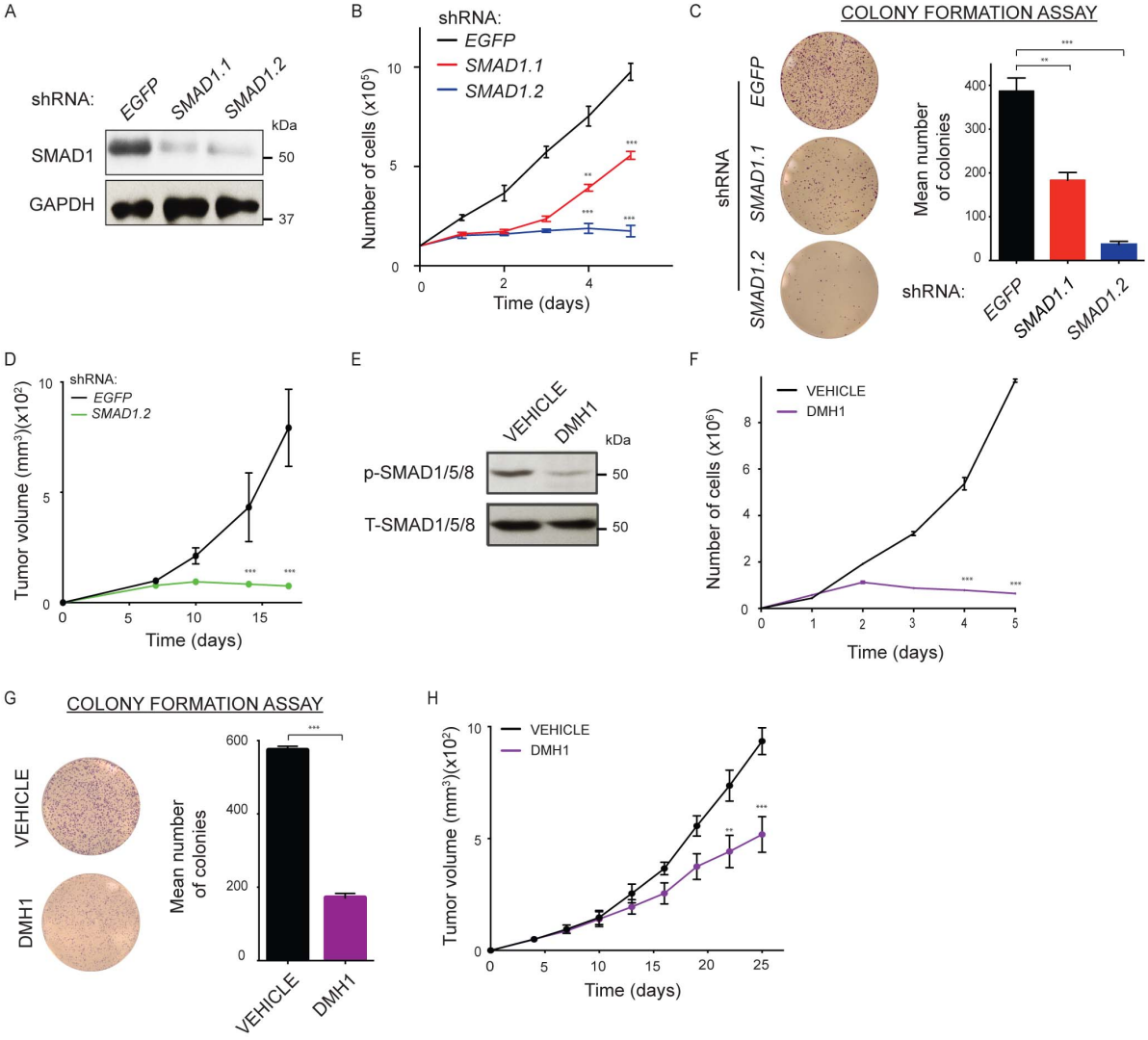

Fig. S6. Inhibition of BMP signaling affects A375 melanoma cell growth

(A) Immunoblots of A375 melanoma cells expressing *shEGFP*, *shSMAD1.1* or *shSMAD1.2*. **(B)** Growth curves of A375 cells expressing *shEGFP*, *shSMAD1.1* or *shSMAD1.2*. **(C)** Colony formation assay with A375 cells expressing *shEGFP*, *shSMAD1.1* or *shSMAD1.2*. **(D)** Tumor formation in mice injected with A375 cells expressing *shEGFP* or *shSMAD1.2*. **(E)** Immunoblots showing expression of phospho-SMAD1/5/8 and total SMAD1/5/8 in A375 melanoma cells after treatment with 0.1% DMSO (vehicle) or 10μM DMH1 in 0.1% DMSO. **(F)** Growth curves of A375 cells treated with 0.1% DMSO (vehicle) or 10μM DMH1 in 0.1% DMSO. **(G)** Colony formation assay with A375 cells treated with 0.1% DMSO (vehicle) or 10μM DMH1 in 0.1% DMSO. **(H)** Tumor formation in mice injected with A375 cells treated with vehicle control or 25 mg/kg DMH1 every other day. Error bars indicate s.e.m.; n=3 in B, C, D, F, G; *n*=8 in H. Two-tailed Student's *t*-test, $^{**}P < 0.01$, $^{***}P < 0.001$.

SUPPLEMENTAL FIGURE 7

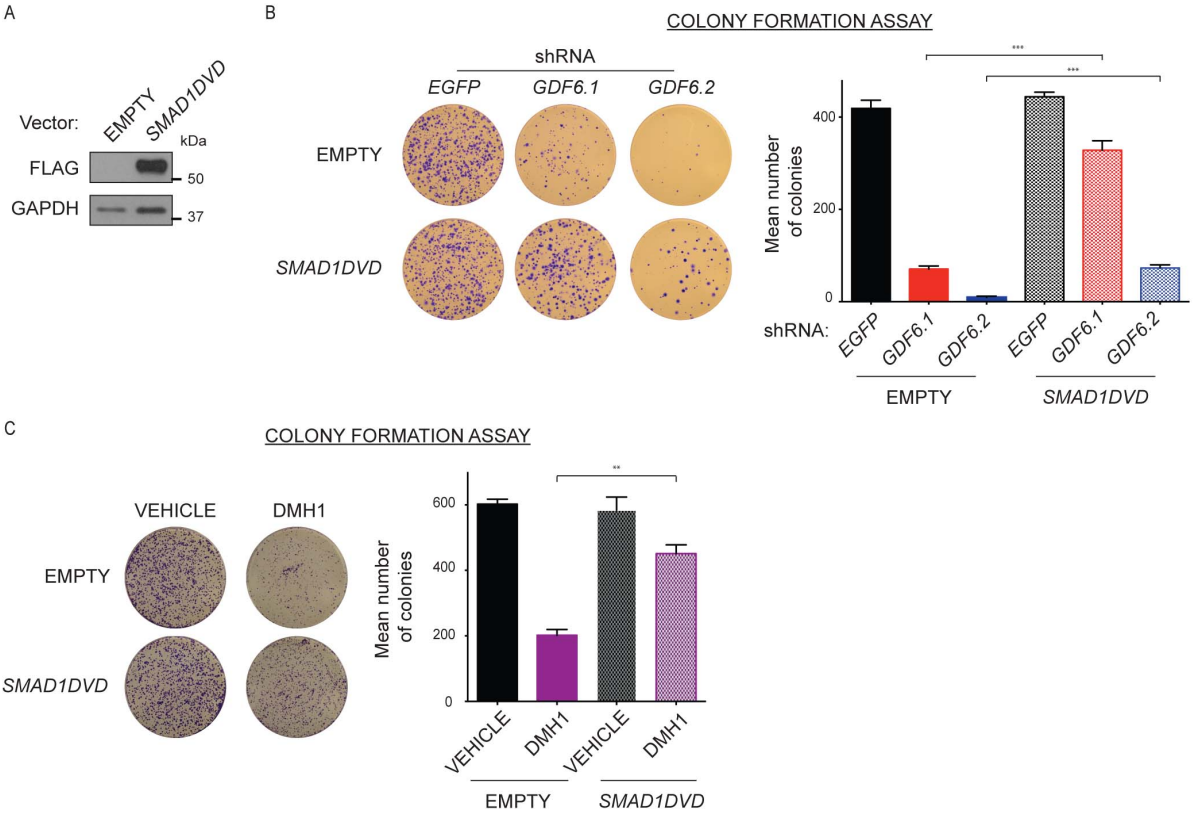

Fig. S7. A375 cell growth defects caused by *GDF6* knockdown or DMH1 treatment are rescued by *SMAD1DVD* expression

(A) Immunoblots of A375 cells overexpressing Flag-tagged *SMAD1DVD*. **(B)** Colony formation assay with A375-EMPTY (top) or A375-*SMAD1DVD* (bottom) cells expressing *shEGFP*, *shGDF6.1* or *shGDF6.2*. **(C)** Colony formation assay with A375-empty or A375-*SMAD1DVD* cells treated with 0.1% DMSO (vehicle) or 10μM DMH1 in 0.1% DMSO. Error bars indicate s.e.m.; n=3. Two-tailed Student's t-test, $^{**}P< 0.01$, $^{***}P< 0.001$.

SUPPLEMENTAL FIGURE 8

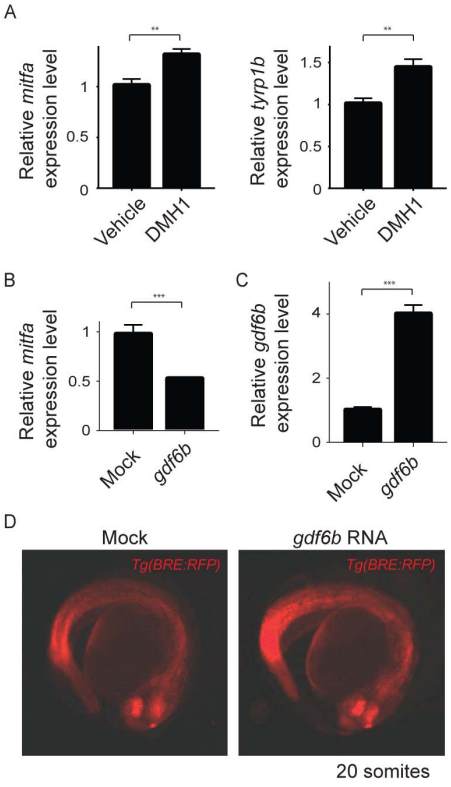

Fig. S8. *gdf6* ortholog and BMP pathway modulation affects expression of melanocyte lineage genes

(A) qRT-PCR showing expression of *mitfa* (left) and *tyrp1b* (right) in 20 somite-stage zebrafish embryos treated with DMSO vehicle control or 10μM DMH1. **(B)** qRT-PCR showing expression of *mitfa* in *gdf6b* RNA or mock-injected 20 somite-stage zebrafish embryos. **(C)** qRT-PCR validating that elevated levels of *gdf6b* RNA are present in 20 somite-stage zebrafish embryos injected with *gdf6b* RNA. (D) BMP pathway activity, as measured by the *Tg(BRE:mRFP)* reporter, is elevated in 20 somite-stage *gdf6b* RNA-injected zebrafish embryos. Error bars indicate s.e.m.; n=3. Two-tailed Student's t-test, $^{**}P< 0.01$, $^{***}P< 0.001$.

SUPPLEMENTAL FIGURE 9

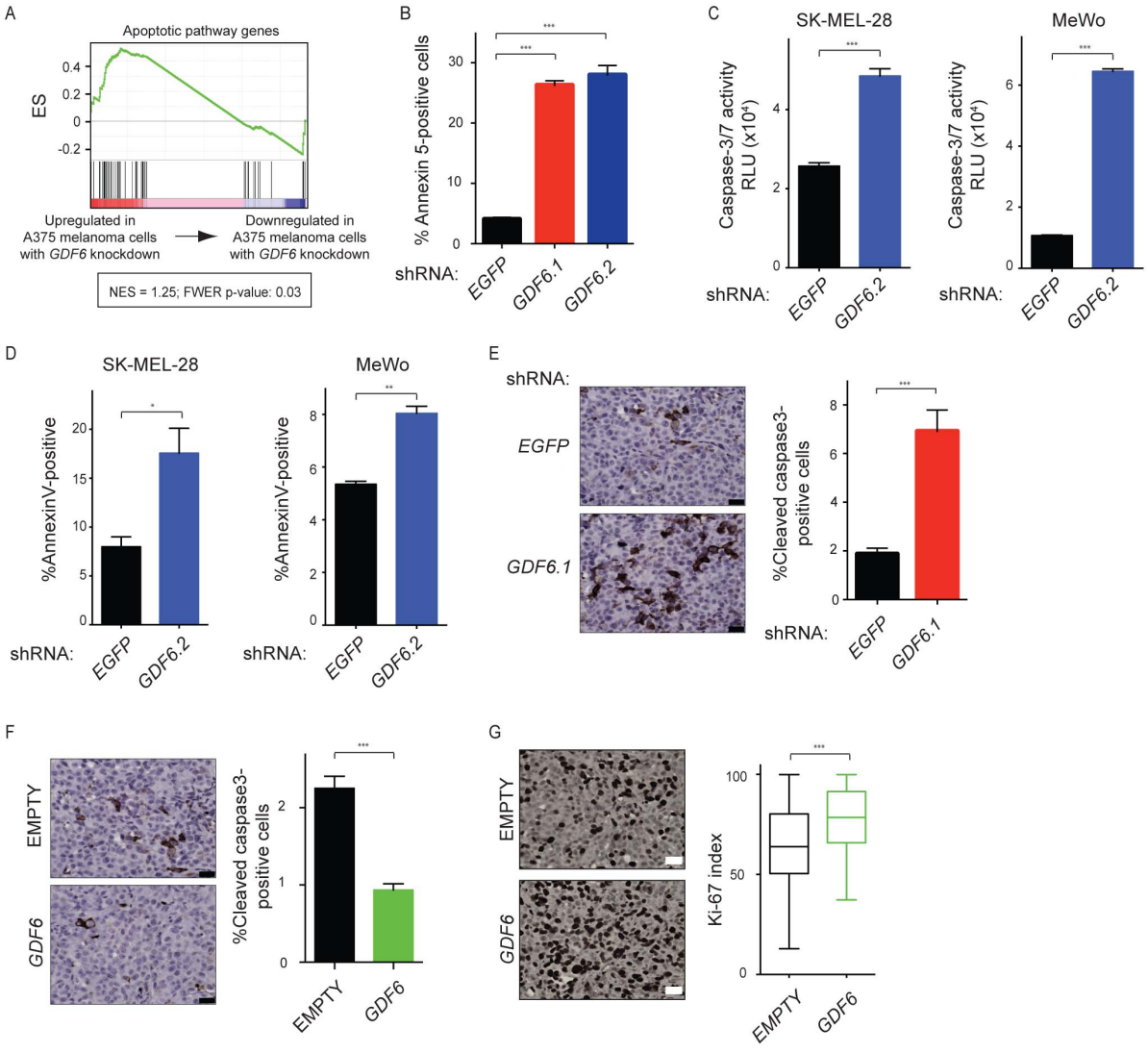

Fig. S9. *GDF6* modulation affects melanoma cell survival

(A) GSEA shows that expression of an apoptotic gene set (*15*) is positively enriched in *GDF6*-knockdown A375 cells **(B)** Flow cytometry analysis of annexinV-positivity of A375 cells expressing an shRNA targeting *EGFP* or two independent *GDF6*-targeted shRNAs. **(C)** Caspase-3/7 activity measured as relative luciferase units (RLU; Caspase-Glo assay) in SK-MEL-28 cells (left) and MeWo cells (right) expressing an shRNA expressing *shEGFP* or *shGDF6.2*. **(D)** Flow cytometry analysis of annexinV-positivity of SK-MEL-28 cells (left) and MeWo cells (right) expressing an shRNA expressing *shEGFP* or *shGDF6.2*. **(E)** Cleaved Caspase-3 staining of mouse xenografts of A375 cells expressing *shEGFP* (top) or *shGDF6.1* (bottom). Scale bar, 25µm. **(F)** Cleaved Caspase-3 staining of mouse xenografts of A375 cells overexpressing empty vector (top) or *GDF6* (bottom). Scale bars, 25µm. **(G)** Ki67 staining of mouse xenografts of A375 cells overexpressing *GDF6* or empty vector control. Scale bar, 25µm.; Error bars indicate s.e.m.; n=3 in B, C, D; n=100 fields in E, F, G. Two-tailed Student's *t*-test, **P*< 0.05, ***P*< 0.01, ****P*< 0.001.

SUPPLEMENTAL FIGURE 10

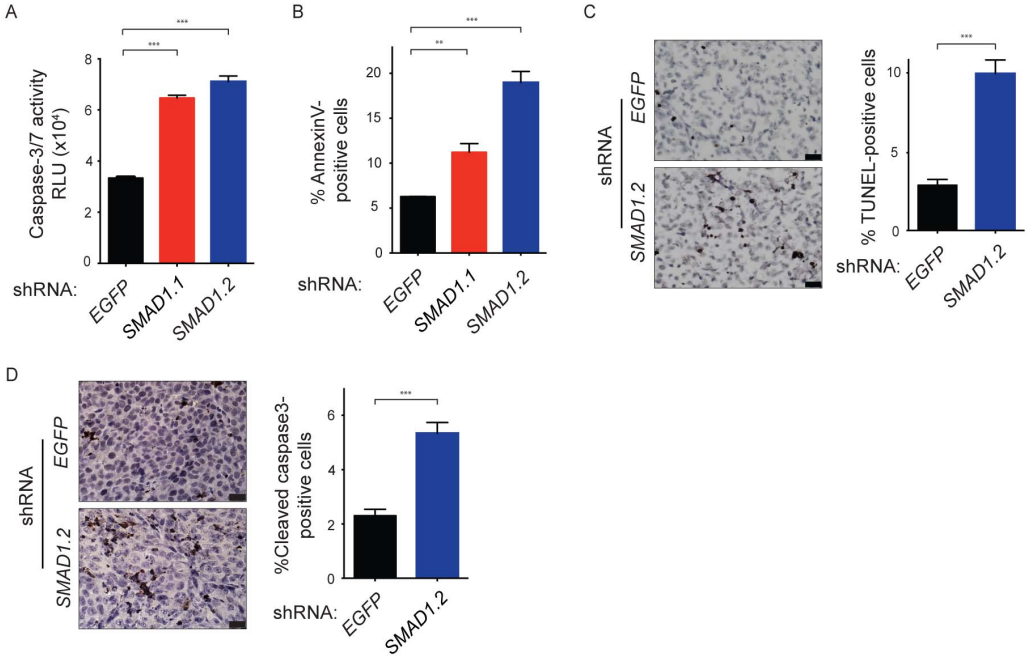

Fig. S10. *SMAD1* knockdown induces apoptotic cell death in A375 melanoma cells

(A) Caspase-3/7 activity measured as relative luciferase units (RLU; caspase-glo assay) in A375 cells expressing an shRNA targeting *EGFP* or two independent *SMAD1*-targeted shRNAs. **(B)** Flow cytometry analysis of annexinV-positivity of A375 cells expressing an shRNA targeting *EGFP* or two independent *SMAD1*-targeted shRNAs. **(C)** TUNEL staining of mouse xenografts of A375 cells expressing *shEGFP* (top) or *shSMAD1.2* (bottom). Scale bar, 25μm. **(D)** Cleaved Caspase-3 staining of mouse xenografts of A375 cells expressing *shEGFP* (top) or *shSMAD1.2* (bottom). Scale bar, 25μm. Error bars indicate s.e.m.; n=3 in A, B; n=100 fields in C, D. Two-tailed Student's *t*-test, $^{**}P < 0.01$, $^{***}P < 0.001$.

SUPPLEMENTAL FIGURE 11

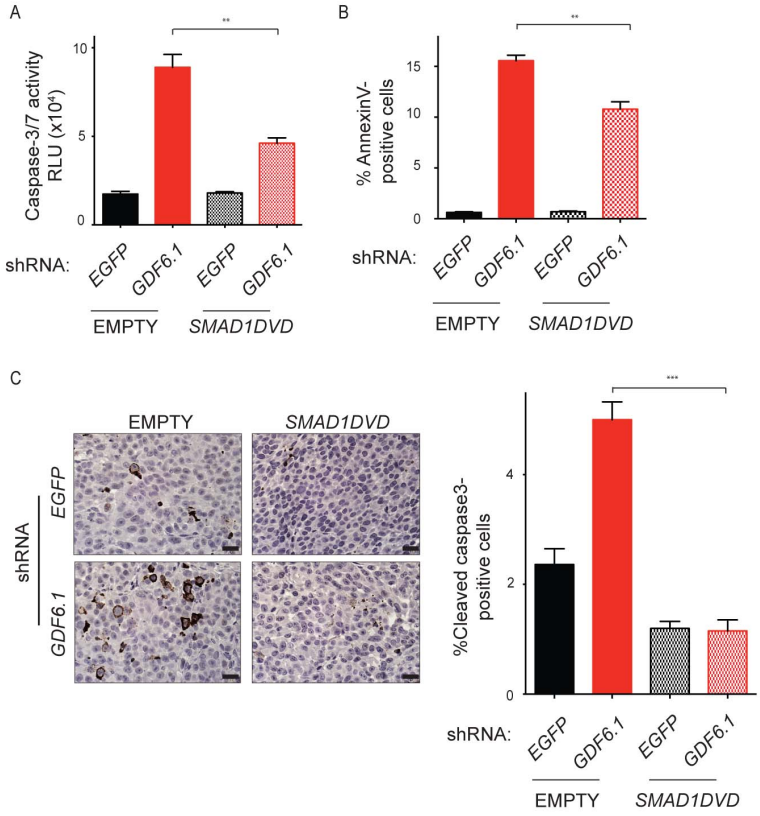

Fig. S11. A375 melanoma cell death caused by *GDF6* knockdown is rescued by *SMAD1DVD* expression

(A) Caspase-3/7 activity measured as relative luciferase units (RLU; caspase-glo assay) in A375-empty or A375-*SMAD1DVD* cells expressing *shEGFP* or *shGDF6.1*. **(B)** Flow cytometry analysis of annexinV-positivity of A375-empty or A375-*SMAD1DVD* cells expressing *shEGFP* or *shGDF6.1*. **(C)** Cleaved Caspase-3 staining of mouse xenografts of A375-empty or A375-*SMAD1DVD* cells expressing *shEGFP* or *shGDF6.1*. Scale bar, 25μm. Error bars indicate s.e.m.; n=3 in A, B; n=100 fields in C. Two-tailed Student's *t*-test, $^{**}P< 0.01$, $^{***}P< 0.001$.

SUPPLEMENTAL FIGURE 12

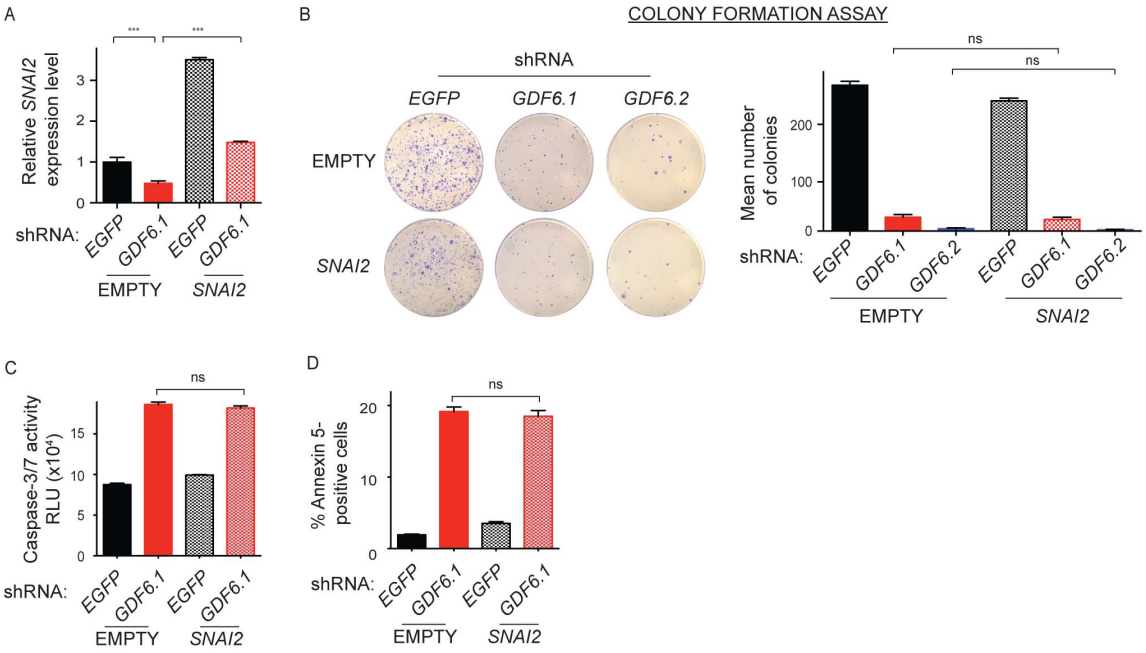

Fig. S12. *SNAI2* expression does not rescue the A375 melanoma cell growth defects and death caused by *GDF6* knockdown

(A) qRT-PCR showing expression of *SNAI2* in A375-empty or A375-*SNAI2* cells expressing *shEGFP* or *shGDF6.1*. Left bracket, *SNAI2* expression is downregulated upon *GDF6* knockdown. Right bracket, *SNAI2* overexpression in *GDF6* knockdown cells. **(B)** Colony formation assay of A375-empty (top) or A375-*SNAI2* (bottom) cells expressing an shRNA targeting *EGFP* or two independent *GDF6*-targeted shRNAs. **(C)** Caspase-3/7 activity measured as relative luciferase units (RLU; caspase-glo assay) in A375-empty or A375-*SNAI2* cells expressing *shEGFP* or *shGDF6.1*. **(D)** Flow cytometry analysis of annexinV-positivity of A375-empty or A375-*SNAI2* cells expressing *shEGFP* or *shGDF6.1*. Error bars indicate s.e.m.; n=3. Two-tailed Student's *t*-test, ***$P < 0.001$. ns, not significant.

SUPPLEMENTAL FIGURE 13

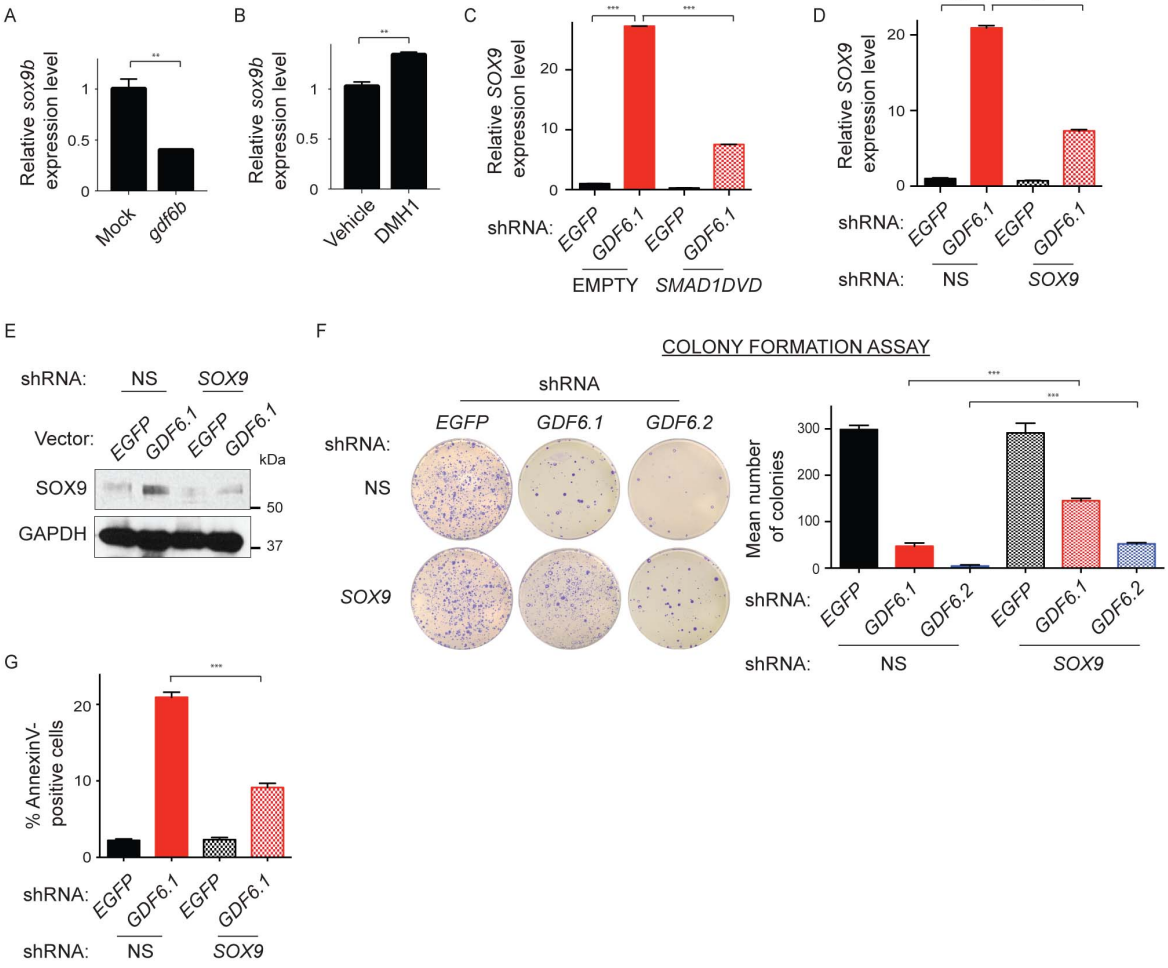

Fig.

S13. *GDF6* and BMP signaling act via *SOX9* repression to aid in melanoma cell survival

(A) qRT-PCR showing expression of *sox9b* in *gdf6b* RNA or mock-injected zebrafish embryos. **(B)** qRT-PCR showing expression of *sox9b* in zebrafish embryos treated with DMSO vehicle control or 10μM DMH1. **(C)** qRT-PCR of *SOX9* in A375-empty or A375-*SMAD1DVD* cells with *GDF6* knockdown. Left bracket, *SOX9* expression is upregulated upon *GDF6* knockdown. Right bracket, *SOX9* expression is less upregulated in *SMAD1DVD*-expressing cells upon *GDF6* knockdown. **(D)** qRT-PCR showing expression of *SOX9* in A375-non-silencing or A375-*shSOX9* cells with *GDF6* knockdown. Left bracket, *SOX9* expression is upregulated upon *GDF6* knockdown. Right bracket, knockdown of *SOX9* expression in *GDF6* knockdown cells. **(E)** Immunoblots showing expression of SOX9 and GAPDH in of A375-non-silencing or A375-*shSOX9* cells expressing *shEGFP* or *shGDF6.1*. **(F)** Colony formation assay with A375-non-silencing (top) or A375-*shSOX9* (bottom) cells expressing an shRNA targeting *EGFP* or two independent *GDF6*-targeted shRNAs. (G) Flow cytometry analysis of annexinV-positivity of A375-non-silencing or A375-*shSOX9* cells expressing *shEGFP* or *shGDF6.1*. Error bars indicate s.e.m.; n=3. Two-tailed Student's *t*-test, ***$P < 0.001$. NS, non-silencing

SUPPLEMENTAL FIGURE 14

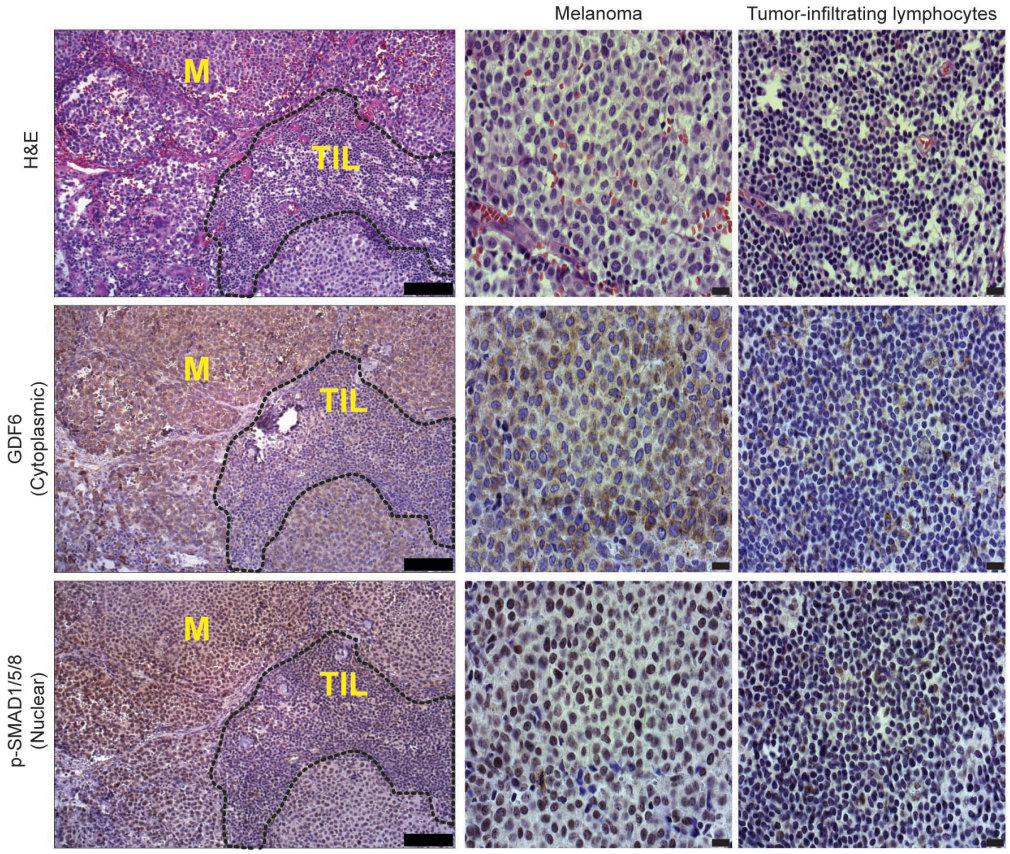

Fig. S14. GDF6 and phospho-SMAD1/5/8 expression in a patient melanoma section

Sections of a metastatic human melanoma with tumor-infiltrating lymphocytes (TIL). Top, hematoxylin and eosin staining. Middle, GDF6 staining. Bottom, phospho-SMAD1/5/8 staining. Left, low magnification. Scale bar, 50 μm. Center, melanoma region, and, right, TIL region. Scale bar, 25 μm.

SUPPLEMENTAL FIGURE 15

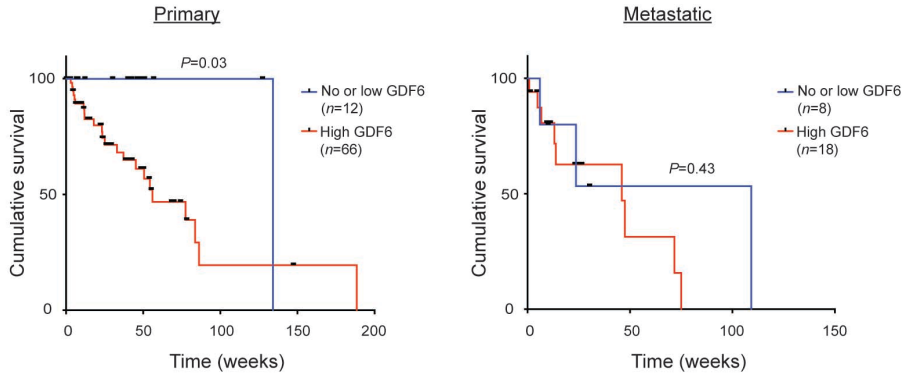

Fig. S15. Correlation of GDF6 expression with melanoma patient survival

Kaplan-Meier analysis showing overall survival of patients with primary melanomas (left) and metastatic melanomas (right) that have no or low GDF6 expression (blue line) versus high GDF6 expression (red line).